doi.org/10.1002/cctc.202001141

Recent Advances in Heterogeneous Catalysis for Ammonia Synthesis

Vijaykumar S. Marakatti*[a] and Eric M. Gaigneaux[a]

Even after a century, ammonia (NH_3) synthesis from nitrogen and hydrogen through Haber-Bosch process is still energy intensive. Even with recently introduced second generation Ru based catalysts with superior performance over commercial Fe based catalysts, there is still place for upgrading with new approach using advanced materials in catalyst formulation. The alkali and alkaline metal promoted Ru supported carbon and metal oxide catalyst attracted attention at initial stage and extensively studied for NH_3 synthesis in the 20th century. Until recently, advanced materials such as electrides, hydrides, nitrides, oxides and oxy-hydrides-nitrides studied as support and active component of catalyst fascinated much attention, with milder reaction conditions for NH_3 synthesis. These materials with unique properties of reversible storage of electrons, hydrides, nitrides and oxygen vacancies enrich electron density on Ru catalyst and cleave N≡N bond with very low activation energy (<60 kJ/mol). The mechanistic understanding of these materials leads to the fact that activation N≡N bond is no more rate-determining step (RDS). Instead, formation of N–H bond is RDS, pushing towards an innovative research directions and scientific basis for development of new catalysts. Enormous maturation of experimental and theoretical methods with improved precession over worldwide research effort helped in gaining a fundamental understanding of these materials in NH_3 synthesis. The most of Ru supported on these advanced materials were better in performance compared to benchmark Cs–Ru/MgO and Ru/AC catalysts in NH_3 synthesis. Insights on these materials and their mechanism are covered in this review, which digs towards finding a realistic catalyst for NH_3 synthesis.

1. Introduction

Ammonia (NH_3) is an essential agricultural feedstock along with industrial, household chemicals, and a precursor for hydrogen storage with upcoming alternative fuel.[1] The foremost use of NH_3 is in production of synthetic fertilizers, which assist in high yield of nutrients crops.[2,3] Therefore, demand for NH_3 production continues to increase to support growing global population with affordable food supply and as carbon neutral fuel. Despite shortcoming, such as high-energy use (28–166 GJ per ton NH_3), process complexity, CO_2 gas emission (1.87 ton per ton NH_3), there remains no alternative to the Haber-Bosh process (HBP).[1,4] In HBP, a mixture of N_2 and H_2 passes over a Fe based catalyst promoted with K_2O and Al_2O_3 at high temperatures (400–600 °C) and pressures (20–40 MPa), consuming more than 1% of the world's power production.[5] Therefore, reduction of N_2 to NH_3 under mild conditions is one of the most challenging topics in catalysis.[6] Cleavage of stable N≡N bond (945 kJ mol) is a significant step in NH_3 synthesis and demands high-energy input. Even after 100 years of discovery, the same old high energy consuming Fe based catalytic process is still operating commercially. The substitute to HBP through dynamic heterogeneous catalyst development remained a Never-Ending Story.[7] The absence of significant success towards a further development of Fe based catalysts stipulates to look at alternative completely different catalysts. In this regard, Ruthenium (Ru) based catalysts supported on carbon emerged as second-generation catalysts for the NH_3 synthesis at the end of 20th century.[8] The special type of B_5 sites in Ru nanoparticles are the active centers for N_2 cleavage at low temperature.[9–12] (Scheme 1) Hence, NH_3 synthesis is considered as a structure sensitive reaction over Ru catalyst.[13] The activity of Ru catalysts considerably enhanced by electron injection from alkali or alkaline earth metal oxide promoters.[14,15] Increased electron density on Ru transfers electrons to antibonding π*-orbitals of N_2 that results in weakening of N≡N bond and promotion of N≡N cleavage. (Scheme 1) As result, wide variety of Ba, Cs promoted metal oxide, carbon supported Ru catalysts with different particle size and morphology were developed for efficient activation of N_2.[16] Amongst, Cs–Ru/MgO is considered as a benchmark catalyst with excellent NH_3 synthesis.[17,18] However, NH_3 synthesis commensurate with increase in pressure is not expected in conventional Ru-based catalysts because of severe hydrogen poisoning on Ru surfaces.[19] This is a major reason why Fe-based catalysts used in HBP has not been replaced by Ru catalyst.

High cost of Ru for commercialization is another factor to consider. Nevertheless, advanced formulated Ru based catalysts with exceptional high efficient in NH_3 synthesis could overcome these barriers. With this belief, new materials established as supports and active catalysts in recent years. The hydrides and electrides supports with tremendous reversible hydrogen and electron storage were found to enhance electron density on Ru and inhibit H_2 poisoning at high pressure.[19,20] Remarkably exhibited low N_2 activation energy with, formation of NH_x as rate determining step (RDS) and not activation of N_2, these studies drive lot of curiosity and scientific basis for design of new catalysts.[19] Another class of materials, ternary nitrides with low-cost and exchangeable lattice nitrogen that can efficiently activate N_2 through Mars van Krevelen mechanism encourages new catalytic prospective.[21] Furthermore, attempts were also made to combine both nitrides and hydrides to form nitrides-hydrides catalyst with more efficient NH_3 synthesis.[22] Consequently, understanding the mechanism behind newly developed catalysts is important for designing low cost highly efficient NH_3 catalyst. There are handful reviews available a way back, covering Ru, Fe, nitrides based catalysts.[4,16,21,23–25] Recently, Chen et al. concisely reviewed hydrides in thermocatalytic ammonia synthesis at milder reaction conditions.[3,26] To our knowledge, there are no reviews covering mechanism of lately developed heterogeneous catalysts for NH_3 synthesis in details and will be considered in this review. The review first sorts the compiled formulations based on properties of

[a] Dr. V. S. Marakatti, Prof. E. M. Gaigneaux
Institute of Condensed Matter and Nanosciences (IMCN)
Molecular chemistry, Solids and caTalysis(MOST)
Université catholique de Louvain (UCLouvain)
Louvain-la-Neuve BE-1348 (Belgium)
Fax: +32 (0)10 47 36 49
E-mail: vijaykumar.marakatti@uclouvain.be

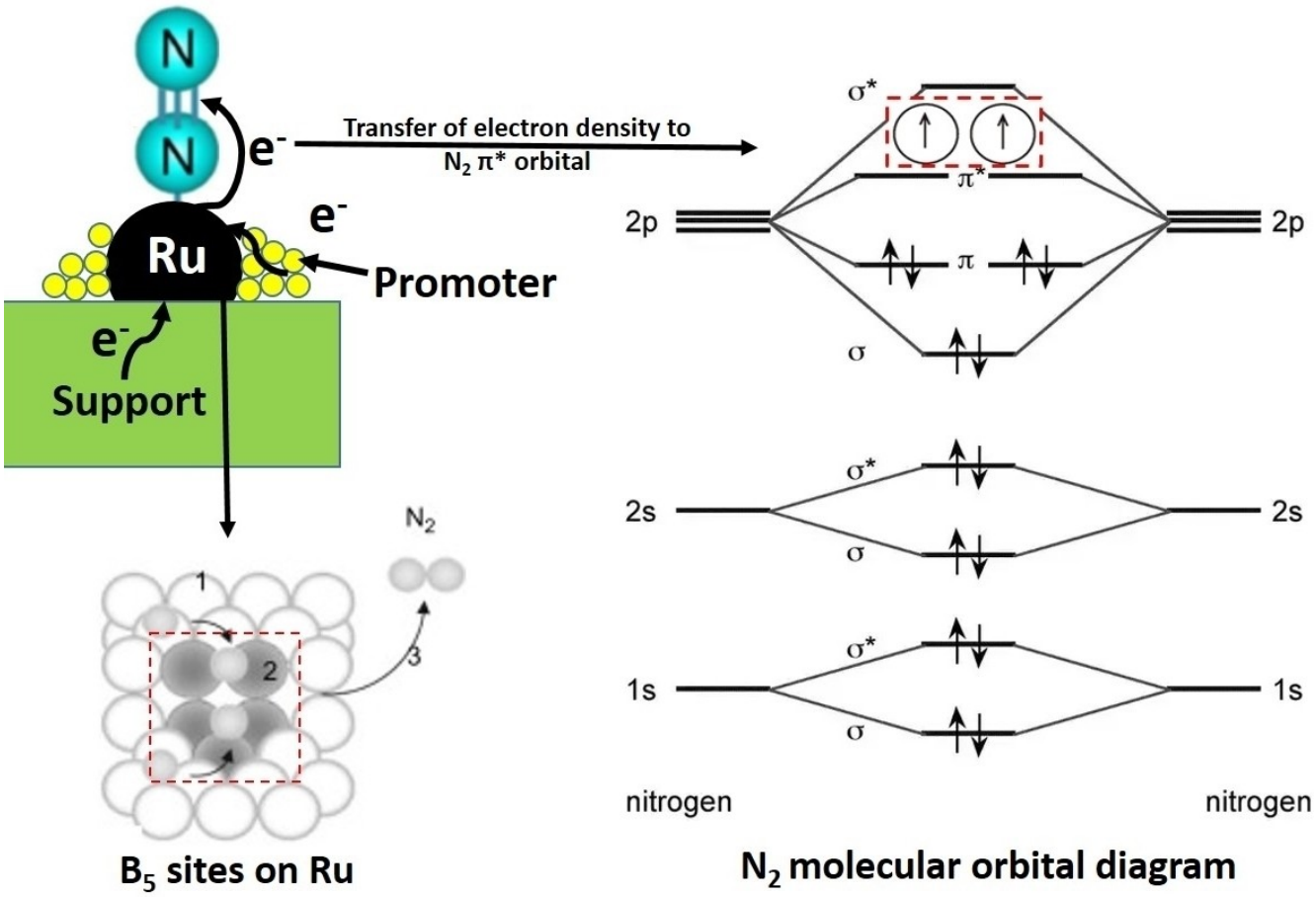

Scheme 1. Electron flow transfer from promoter, support to B_5 active site of Ru and then to π^* orbital of N_2 with reduced bond order as seen from the Molecular orbital diagram.

materials into electrides, hydrides, nitrides, oxides, intermetallic/alloys and other supported catalysts, and each is discussed in the subsequent sections followed by summary and outlook. A separate table created for each family of active catalysts for the easy understanding of the experimental details and comparisons of catalysts. The review will give insights on recent development on these materials and their mechanism, even-

Dr. Vijaykumar Marakatti obtained Ph.D (2015) from PoornaPrajna Institute of Scientific Research (PPISR), Bengaluru, India. Later, he moved to Dr.Sebastian C. Peter group at Jawaharlal Nehru Centre for Advanced Scientific Research (JNCASR), Bengaluru as "National Postdoctoral Fellow (NPDF)" (2015–17). He joined Prof. Eric M. Gaigneaux group at UCLouvain, Belgium as FSR-FNRS Postdoctoral Fellow (2017-19) and is currently a Marie Skłodowska Curie Postdoctoral Fellow (2019–21). His research work focusses on development of Nano intermetallic and alloy supported catalysts for NH_3 synthesis, CO_2 to value added chemicals, and biomass conversions.

Dr. Eric Gaigneaux is Professor at Institute of Condensed Matter and Nanosciences (IMCN), Université catholique de Louvain (UCLouvain), Belgium. His main scientific interests are the preparation of heterogeneous catalysts with a control of their morphology at the atomic and nanoscopic scales, their physico-chemical characterization under operational in situ/operando conditions, and their applications in the production of biofuels, abatement of air and water pollutants, transformation of light hydrocarbons and alcohols to more valuable molecules via selective oxidation, ammoxidation, dehydration and oxidative dehydrogenation, hydrogenation of nitrogen to ammonia, and fine chemistry with a particular interest for epoxidation, Friedel-Crafts reactions and the oxidative cleavage of unsaturated fatty acids.

tually broadening the views and ideas towards finding a realistic catalyst for NH_3 synthesis.

2. Different class of catalysts for NH_3 synthesis

2.1. Electrides

Electrides are materials with electrons trapped in their structural cavity and serve as anions.[20] Most of organic electrides are chemically and thermally unstable and decompose at room temperature.[27] The first stable inorganic electride in air and room temperature was C12A7:e^- synthesized from $12CaO.7Al_2O_3$(C12A7). C12A7:e^- is made of positively charged C12A7 framework connected by O^{2-} ions to maintain electroneutrality.[28,29] (Figure 1.a) In such structure, two of the O_2^- ions can be substituted by four electrons with chemical modification and final chemical formula is expressed as $[Ca_{24}Al_{28}O_{64}]^{4+}(e^-)^4$.[19] At outset, this may appear similar to F^+ centers i.e crystallographic defects, where unpaired electrons occupy anionic vacancy in a crystal lattice. However, such F^+ centers have high potential barrier for electron transfer, low surface electron concentration and are prone of structure alteration.[19] While, C12A7:e^- is a three-dimensional structure with unique 'cage conduction band' and thin cage walls possessing conduction similar to metals.[30] (Figure 1.b) The conduction properties in C12A7:e^- is controlled by the concentration of electrons in cages, 50% and lower substitution of O_2^- by electrons make C12A7:e^- a semiconductor and further increased substitution (more than 50%) turns on metallic conductivity.[31] Such efficient electrons transfer to Ru nanoparticle on the surface of C12A7:e^- improves the dissociation for N_2. Another compelling property of C12A7:e^- that assist in NH_3 synthesis is ability of reversible hydride storage i.e. electrons encapsulated in cages of C12A7:e^- are replaced readily by hydride ions (H^-), avoiding inhibition of Ru surface by hydrogen under high pressure.[32] These two unique properties of high electron tunneling and reversible H^- storage make C12A7:e^- a potential catalytic support for NH_3 synthesis.

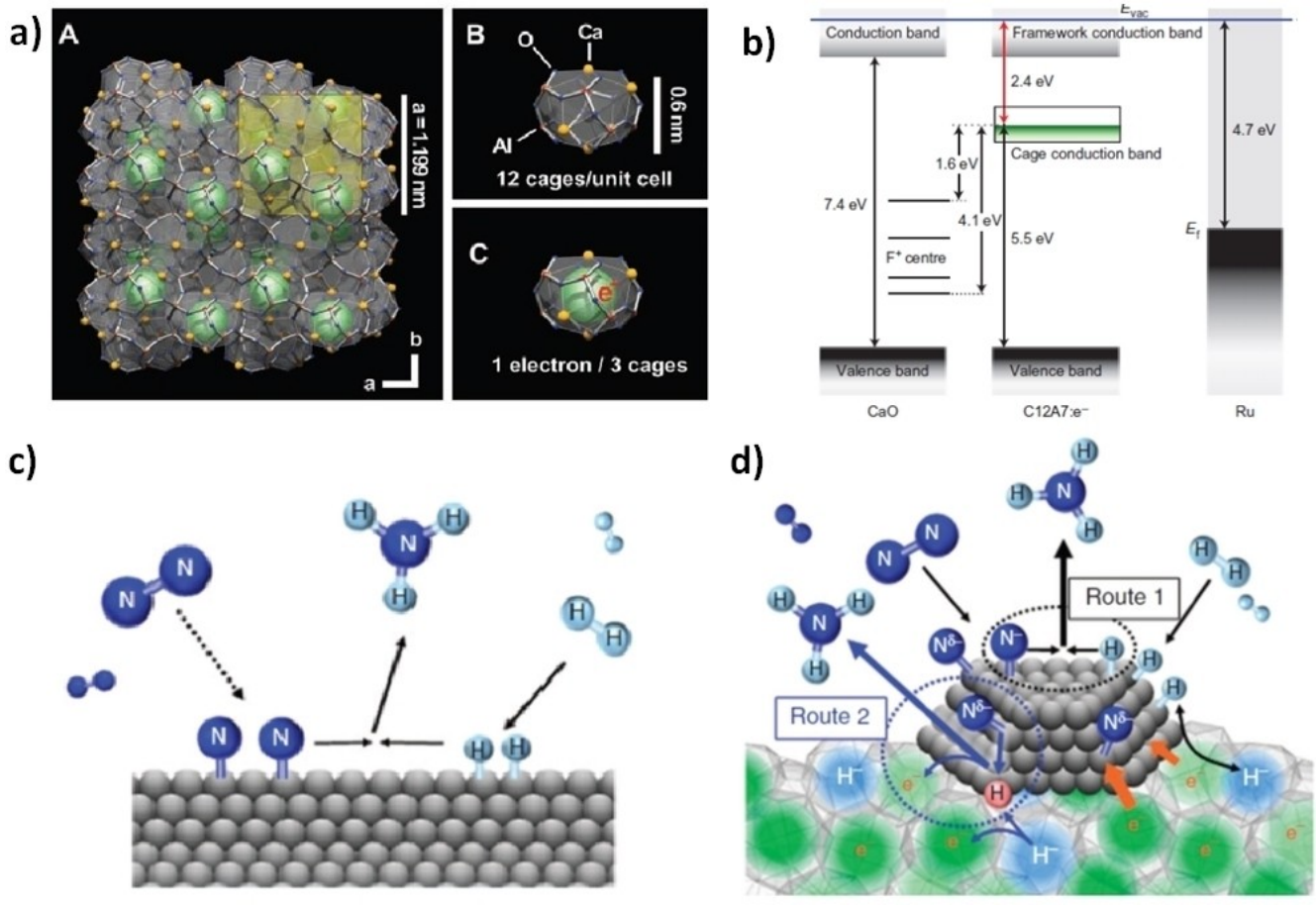

Figure 1. a) Crystal structure of $[Ca_{24}Al_{28}O_{64}]^{4+}(e^-)^4$. The framework of stoichiometric C12A7 is composed of 12 cages. Two out of 12 cages are occupied by O_2^- ions, Cages are occupied by electrons in place of O_2^- ions.[28] Reproduced with permission from Ref. [28]. Copyright 2003, American Association for the Advancement of Science **b)** Comparison of the energy levels for a F^+ center in CaO, CCB in C12A7:e^- and the Fermi level (Ef) in Ru. Reaction mechanism **c)** through a Langmuir-Hinshelwood mechanism to form NH_3 in which N_2 dissociation is the RDS which occurs in Ru/C12A7:e^- at low temperature of 300 °C . **d)** Ru/C12A7:e^- the rate-limiting step is formation of N–H_n species. NH_3 is formed through the Langmuir-Hinshelwood mechanism (route 1) and the direct reaction of N adatoms with H radicals (nascent hydrogen) derived from cage H^- anions (route 2)[19] Reproduced with permission from Ref. [19] Copyright 2012 Springer Nature.

In 2012, Ru/C12A7: e^- catalyst synthesized by Hosono group displayed higher catalytic activity compared to commercial Ru–Cs/MgO, Ru/CaO, Ru–Ba/Activated Carbon(AC) catalysts in NH_3 synthesis.[19] (Table 1, Entry 1–6) C12A7: $(O^{2-})_2$ without electrons in the cages is a typical band insulator and shows lower activity.[31] Ru/C12A7:e^- exhibited high NH_3 synthesis rate and turn over frequency (TOF) even at low temperature with least activation energy compared to reported conventional catalysts. (Table 1, Entry 1–6) Moreover, Ru/C12A7:e^- catalyst exhibits excellent stability under high pressure with time on stream of 75 h. The pressures dependent studied suggest the TOF of Ru/C12A7:e^- increases with pressure from 0.1 to 1 MPa, whereas conventional Cs–Ru–/MgO exhibits TOF independent to total pressure due to selective poisoning of H_2 preventing the N_2 activation. These studies confirm potential capability of electride materials as catalysts for industrial application.[19]

The cause for high activity of Ru/C12A7:e^- was resolved through kinetic, spectroscopic and isotopic experiments. Chemisorbed N_2 on Ru/C12A7:e^- displays vibrational peaks at lower wavenumber (2194 cm^{-1}) compared with conventional Ru catalyst (2245 cm^{-1}) demonstrating weakened $N\equiv N$ bond through effective electrons transfer from electride to Ru and then to antibonding orbitals of N_2.[29] Additionally, kinetic studies reveal N_2 order of reaction is low (~0.46) for Ru/C12A7: e^- compared to conventional Ru catalysts (0.8~1) signifying efficient N_2 dissociation on electride catalysts.[32] Low order of reaction for N_2 along with kinetic N_2 exchange isotope studies suggests dissociated N adatoms are constantly available on the surface for reaction, making N_2 cleavage not a RDS anymore.[24]

The high poisoning effect of H_2 on conventional Ru catalysts is understood from their negative H_2 order of reaction (−0.3 to −1.2) but this turned to be positive (+1) for Ru/C12A7:e^-. Low H_2 inhibiting effect for Ru/C12A7:e^- is due to the surface reaction of dissociated H atoms (spill over H atoms) with cage electrons of electrides to form H^- ions. ($H^0 + e^- \rightarrow H^-$). However, complete (100%) substitution of cage electrons by H^- is not possible and exchange is limited to only 4%. These extra-framework hydride ions formed in close proximity to Ru particles at the cages, later regenerate back to H atoms (leaving the cage electrons) which then react with N adatoms on Ru, resulting in NH_3.[29] This reversible H^- storage-release phenomenon over Ru/C12A7:e^- is highly efficient at 400 °C, but decays at low temperature (300 °C), where NH_3 synthesis over Ru/C12A7:e^- proceeds similar to conventional Ru catalyst with high activation energy.[32] Therefore, dissociative H_2 adsorption proceeds simultaneously with N_2 cleavage, increasing concentration of H adatoms on Ru surface and part of H adatoms moves into C12A7: e^- to provide a balance between H^- storage reaction and H release reaction. This dynamic mechanism makes it possible to keep high cage electron density and high catalytic performance. Hence, RDS in Ru/C12A7:e^- catalyst is formation of N–H species and not the N_2 activation.[19]

Table 1. Physiochemical properties and catalytic activity in NH_3 synthesis over different electride catalysts. (Reaction Conditions: Catalyst = 0.10/0.2 g, H_2: N_2 = 3:1, total flow = 60 ml/min, Pressure = 0.1 MPa.)

Entry	Catalyst	Ru Loading [wt %]	Surface Area [m^2/g]	Particle Size [nm]	Temperature [°C]	NH_3 yield [$\mu mol/g_{cat}/h$]	TOF [s^{-1}]	Ea [kJ/mole]	Ref
1	Ru/C12A7:e^-	1.2	~1	41.3	400(350)	2757(838)	0.197	49.1	[19]
2	Ru/C12A7:e^-	0.1	~1	8.5	400(350)	715	0.161	53.6	[19]
3	Ru/C12A7:O_2^-	1.2	~1	39.2	400(350)	546(59)	0.038	104.6	[19]
4	Cs–Ru/MgO	1.0	12	2.7	400(350)	2264(618)	0.013	85.8	[19]
5	Ba–Ru/AC	1.0	310	5.3	400(350)	148(14)	0.003	88.8	[19]
6	Ru/CaO	1.5	3.0	27.2	400(350)	158(12)	0.006	120.1	[19]
7	Ru/C12A7:e^- (HT)	2.0	23	9.0	340	2290	0.0239	53.0	[33]
8	Ru/C12A7:e^- (SP)	2.0	~1	42	340	1080	0.0575	49.0	[33]
9	Co/C12A7:e^-	2.6	–	3.7	340	912	0.00213	49.5	[34]
10	Ru/C12A7_$RuCl_3$	2.0	–	–	400	3053	–	–	[35]
11	Ru/C12A7_$Ru_3(CO)_{12}$	2.0	–	–	400	3010	–	–	[35]
12	Ru/Ca_2N:e^-	1.8	1.5	42.8	300(340)	1674(3386)	91.5	60	[36]
13	Ru/CaNH	1.8	1.0	30.2	300(340)	53(308)	2.0	110	[36]
14	Ru/C12A7:e^-	1.8	1.0	28.7	300(340)	745(2021)	24.9	51	[36]
15	Cs–Ru/MgO	2.0	3.8	10.9	300(340)	697(3200)	4.2	120	[36]
16	Ru/CaH_2	2.0	12.0	2.5	300(340)	2549(4002)	98.0	51	[36]
17	Ru/CaH_2	10	20	2.7	340	7400	0.004	68	[37]
18	Ru/BaH_2	10	13	2.7	340	200	–	44	[37]
19	Ru/BaO/CaH_2	10	20	4.0	340	10500	0.0092	41	[37]
20	Ru/Y_5Si_3	7.8	2.0	–	400	1900	0.07	52	[38]
21	Cs–Ru/MgO	6.0	12	–	400	3400	0.008	–	[38]
22	Ba–Ru/AC	9.1	310	–	400	2200	0.003	–	[38]
23	Ru/LaScSi	1.8	2-3	–	400	2800	0.1	52	[39]
24	Ru/LaScSi	8.3	2-3	–	400	3400	0.07	49	[39]
25	LaCoSi	–	1.8		400	1250	–	42	[40]
26	Co_3Mo_3N	–	8.5	–	400	796	–	59	[40]
27	Fe–K_2O–Al_2O_3	–	14	–	400	330	–	–	[40]
28	LaRuSi		1.0		400	1760	40.4		[41]
29	CaRuSi		1.8		400	60	–	–	[41]
30	LaRuSi-Before EDTA treatment	–	1.4	–	400(340)	1810(840)	0.060	40	[42]
31	LaRuSi-After EDTA treatment	–	4.2	–	400(340)	5340(3020)	0.059	48	[42]

Based on theoretical calculations and experimental evidences two different mechanisms postulated. The first route is based on classical Langmuir-Hinshelwood mechanism, where both N and H adatoms (generated by H^-) with close proximity on Ru surface react to form N–H bond and then to NH_3. (Figure 1.d route 1) Alternative possibility is direct reaction of N adatoms with H radicals ("nascent H" atoms not bonded to Ru/electride but generated by H^-) as illustrated from Figure 1.d route 2. The strong adsorption of H adatom on Ru (at high pressure) requires high-energy barrier to form N–H (in route 1), in such case reaction of N adatoms with "nascent H" released from H^- is possible, particularly at high pressure (route2). In any case, the formation of transient H^- ions is the important step of NH_3 synthesis over Ru/C12A7:e^-.[32]

Low surface area ($<2\ m^2/g$) of C12A7:e^- by solid state(SS) method stimulates to look for an alternative synthesis method to produce high surface area electride to enhance Ru dispersion and loading. In view of this, C12A7:e^-(HT) with high surface area of $23\ m^2/g$ was synthesized by hydrothermal method.[33] The rate of NH_3 synthesis over Ru/C12A7:e^- (HT) is twice that of Ru/C12A7:e^- (SS), with no significant difference in activation energy.(Table 1, Entry 7–8) Despite high surface area and electron concentration, Ru/C12A7:e^- (HT), exhibited lower (half) TOF than Ru/C12A7:e^- (SP), due to low crystallinity and CaO impurity.[33] The loading of Co metal (considered as another active metal for N_2 activation) on C12A7:e^- displayed good activity but much lower than Ru.[34] (Table 1, Entry 9) The presence of chloride ions in conventional Ru supported catalysts often inhibits electron transfer from support to Ru by virtue of high electron withdrawing property, and hampers catalytic activity.[43,44] But existence of (O_2^-) cages in C12A7 easily encapsulate these Cl^- when $RuCl_3$ is precursor making C12A7 a chlorine tolerant Ru catalyst.[35] (Table 1, Entry 10–11) These unique properties make C12A7:e^- an ideal and efficient support for Ru catalysts in NH_3 synthesis.

Outstanding activity of Ca12A7:e^- is possible only at high temperature (400 °C) and diminishes at low temperature (320 °C) due to rigid Ca–Al–O monolayer with release of hydrogen(stored as hydride) difficult from cages.[32] This shortcoming was overcome by developing a new Ca_2N:e^- electride, which possesses intrinsically low work function, reversible hydrogen-hydride reaction possible at 200 °C and hence strongly promotes NH_3 synthesis on Ru nanoparticles at low temperature.[36,45–47] XRD and Raman spectroscopy revealed Ca_2NH_{1-x} is an active phase during NH_3 synthesis reaction conditions and not $[Ca_2N]^+$:e^- electride. The stable Ru–N bond in Ru/Ca_2NH anchors Ru nanoparticles to the Ca_2NH support with strong metal support interaction(SMSI).[48] With small work function (2.3 eV), electrons confined between positively charged slabs of $[Ca_2N]^+$ layers easily exchange with hydrogen to hydrides and vice versa.[49] (Figure 2.a) With reversible H^- exchange, RDS in NH_3 synthesis is again formation N–H bond and not the dissociation of N_2.[36] Ru/Ca_2NH exhibits high NH_3 synthesis rate and TOF at low temperature (300 °C) compared to Ru/Ca12A7:e^-, Ru/CaNH and Ru–Cs/MgO[36] (Table 1, Entry 12–15). Therefore, pure hydride supports such as Ru/CaH_2 exhibited high catalytic activity due to easy desorption of hydrogen from surface above 200 °C in presence of a Ru catalyst (Table 1, Entry 16).[36] High activity Ru/CaH_2 owing to partial conversion of hydrides to electride by Ru, hence makes Ru/$CaH_{2-x}(e^-)_x$ functioning as electride catalyst.[50] Further adding BaO promoter to CaH_2 generated BaO–BaH_2 layer on the surface of CaH_2. Ru supported on such BaO–BaH_2 layer is more active than CaH_2.[37,51] (Table 1, Entry 17–19) Theoretical studies also report that alloying late and early transitional metals with Ru would promote hydrogen vacancies in Ca_2NH and improve catalytic activity.[52]

Since above discussed electrides are moisture sensitive, a new water resistant electride $[Y_5Si_3]^{0.79+}$:$e^{-0.79}$ was developed for NH_3 synthesis.[38] Y_5Si_3 is an intermetallic compound (IMC) crystalizing as Mn_5Si_3-type structure ($P6_3/mcm$). The quasi-one-

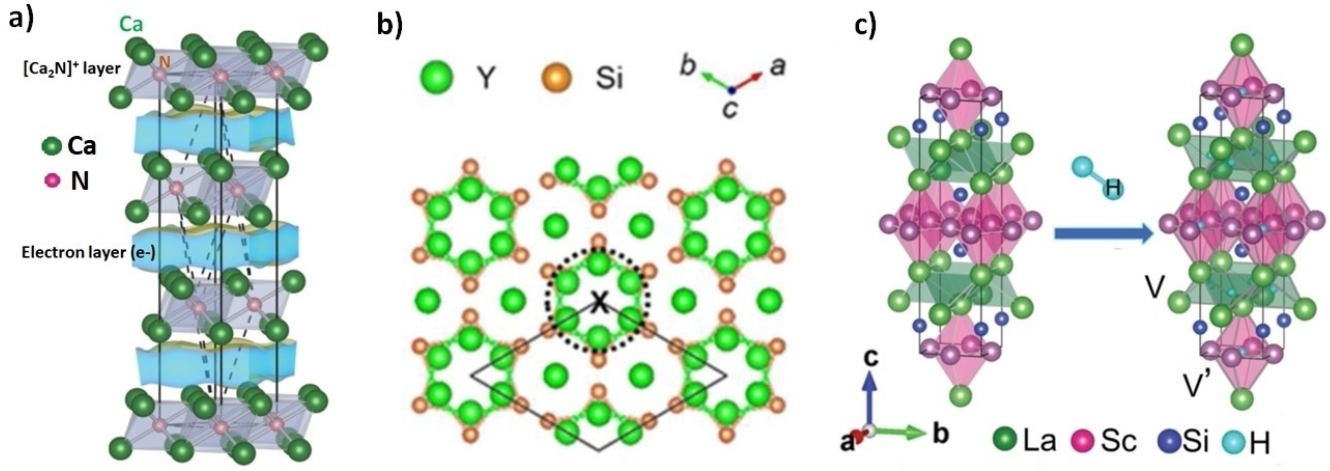

Figure 2. Crystal structure of a) Ca_2N, Ca_2N^+ separated by intermediate electron layers,[46] Reproduced with permission from Ref. [46] Copyright 2012 Springer Nature **b)** Y_5Si_3, interstitial site(X) can accommodate hydrogens[38] Reproduced with permission from Ref. [38] Copyright 2016, American Chemical Society and **c)** LaScSi and $LaScSiH_{1.5}$ with tetrahedral (V) and octahedral voids (V').[39] Reproduced with permission from Ref. [39] 2017 WILEY-VCH Verlag GmbH & Co. KGaA, Weinheim.

dimensional holes (~4 Å) along the c-axis in Y_5Si_3 denoted by X are interstitial sites and accept hydrogen to form Y_5Si_3H. (Figure 2.b) These X sites help in reversible H^- storage ability in Y_5Si_3 as described in other electrides. The TOF for Ru (7.8 wt %)/Y_5Si_3 was several times higher than Cs–Ru/MgO and Ba–Ru/AC, but lower than Ca12A7:e^- and Ca_2N:e^- catalysts.[38] (Table 1, Entry 20–22) The lower activity of Y_5Si_3 electride is due to its low concentration of H content (less than 0.5×1022 cm^{-3}). To enhance high hydrogen exchange capacity, a new class of ternary intermetallic, LaScSi was studied as electride support for NH_3 synthesis.[39] LaScSi has a tetragonal structure (*I*4/*mmm*), with tetrahedral (V) and octahedral (V') voids formed by La_4 and La_2Sc_4 structures, respectively. (Figure 2.c) Without altering structure, electrons can be filled in both the voids. Studies show around 1.5 hydrogen atom can reversible exchange per LaScSi formula unit (f.u). Theoretical calculations suggested around (66.6%) tetrahedral voids (V) are filled first and later the octahedral voids (33.3%) leading to structural formula LaScSiH$_{1.5}$.

With such reversible H^- storage capacity, Ru/LaScSi appears to be a promising catalyst, as indicated by TOF of $\approx$0.1 s^{-1}, one or two orders of magnitude higher than other Ru based catalysts. (Table 1, Entry 23–24) LaScSi was stable even after exposure to water vapor during each run, demonstrating high durability. The high cost scandium makes it again a not good choice for commercial application.

Remarkably, replacement of Sc by Co atom in LaScSi resulted in high NH_3 synthesis rate without loading Ru.[40] LaCoSi differs on the fact that Co and Si are negatively charged unlike in LaScSi where only Si is negatively charged. This could be due to high electropositive nature of Sc.[40] The electron enrichment on Co (−0.37) is promoted by surrounding positively charged La atoms in LaCoSi, this triggers N_2 adsorption through coulombic attractions (Figure 3.a–c) and energy released in such exothermic adsorption process was used for N_2 dissociation ("Hot atom" mechanism). Readily available activated hydrogen atoms stored in the tetrahedral voids of LaCoSi near surface edge reacts with the dissociated N adatom to form N–H and further to NH_3. The specific electronic and geometry of La and Co in LaCoSi is significant for activation of N_2 through hot atom mechanism. LaCoSi exhibited good activity compared to other reported Co_3Mo_3N and commercial Fe catalysts. (Table 1, Entry 25–27) LaSi, La_5Si_3 IMCs with good hydrogen storage capacity compared to LaCoSi show no activity substantiating presence of Co indeed necessary for activation of N_2. LaCoSi displayed excellent stability (100 h) with constant NH_3 synthesis rate unlike binary intermetallic that undergoes quick decomposition.[53] These findings turned intermetallic electrides as a new platform of catalysts for NH_3 synthesis.

A series of RTX IMCs (R-rare earth, T = transition metal, X = Si) with different rare earth and transition element combinations were screened for NH_3 synthesis.[41] LaRuSi and CaRuSi with structures analogous to LaCoSi, differ in their H^- exchange properties, and hence display different catalytic activity.[41] (Table 1, Entry 28–29) Electron rich Ru (−0.55) in LaRuSi exhibits higher electron donation ability and NH_3 synthesis rate compared Co (−0.37) in LaCoSi. Additionally, improving surface area of bulk LaRuSi by ball milling did not enhance catalytic activity due to creation of nanoparticle with exposed La surface layers rather than desired catalytically active Ru layers.[42] To remove surface La layers, treating IMCs with different etching agents (HNO_3, HCl and HCOOH) was executed, EDTA-2Na was effective to create exposed surface with Ru sites. As consequence, catalytic activity of LaRuSi after EDTA treatment enhanced drastically as seen from Table 1. (Entry 30–31). LaRuSi is an example where B_5 sites of Ru are not necessary for NH_3 synthesis.[42] (Figure 3.d)

Overall, studies on different electrides demonstrate essential role of hydride ions in NH_3 synthesis. Therefore, metal hydrides are another potential class of catalysts for NH_3 synthesis. In this direction, limited number of hydrides reported for NH_3 synthesis are deliberated in the next section.

2.2. Hydrides

Hydrides are binary combination of hydrogen and a metal or metalloid, defined as a compound in which there is a metal-to-hydrogen bond.[54] Hydride is the simplest anion, formally H^-, consisting of two electrons and a proton. With reasonably high

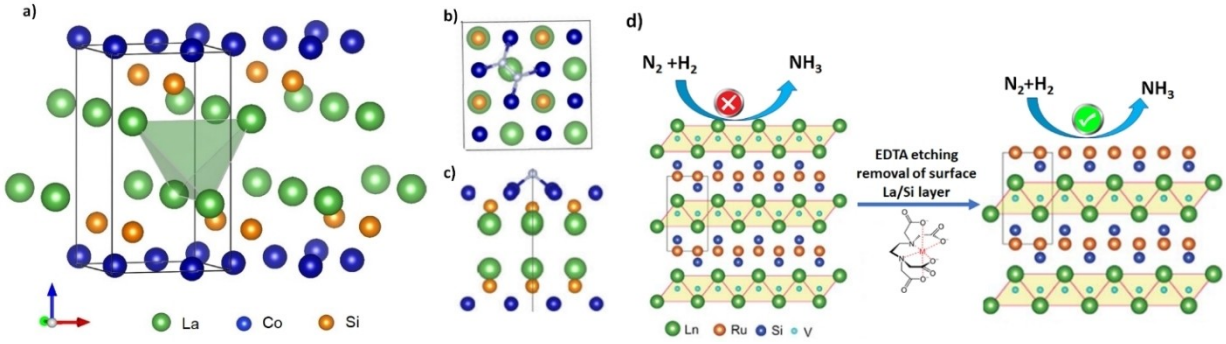

Figure 3. Crystal structure of a) LaCoSi, b) Top and c) Side view of adsorbed bridged N_2 between Co atoms and stabilized by bottom La atom,[40] Reproduced with permission from Ref. [40] Copyright 2018, Springer Nature and d) Etching of LaRuSi with EDTA generating Ru rich layer for NH_3 synthesis.[42] Reproduced with permission from Ref. [42] Copyright 2019 Royal Society of Chemistry.

charge/radius ratio with low electron affinity hydrides are used in chemical reactions as strong reducing agents. Diffusion of the hydride layers toward the bulk is reversible, allowing H^- species to move either to the surface or to the bulk, according to the temperature and pressure.[55] Therefore, the exceptional reducing property and reversible hydrogen storage capacity of hydrides are crucial in a reaction. In 2016, first work on hydrides reported by Chen et al. demonstrating LiH can mediate as second active center along with transitional metal (TM) or metal nitride (TMN) in NH_3 synthesis.[56] Early TM/TMN exhibit excellent N_2 dissociation energy but are less prone for NH_3 synthesis due to accumulation of dissociated N adatoms on surface and lack of active sites for hydrogenation. Nevertheless, addition of LiH has improved NH_3 yield by removing excess N adatoms from surface of TM/TMN with formation of LiNH(imide), which on further hydrogenation regenerates LiH with formation of NH_3 (Figure 4). This way N impoverished surface of TM/TMN further favors N_2 activation and continues with NH_3 synthesis on LiH sites. Kinetic studies suggest transfer of N adatoms from TM/TMN to LiH and further hydrogenation LiNH is RDS and not N_2 dissociation.[56] Intermediate metals Cr, Mn, Fe and Co catalysts mediated with LiH have comparable catalytic activity indicating strong influence of LiH on early and late TM. (Table 2, Entry 1–5) Among different hydrides (NaH, KH, and CaH_2), LiH and BaH_2 are more effective in formation of stable imide (LiNH/BaNH) as consequence a better activity in NH_3 synthesis.[57] (Table 2, Entry 6–11) But studies on Co–BaH_2 catalyst at low temperature illustrate direct activation of N_2 on BaH_2 and further BaNH hydrogenation on Co surface, conflicting to what was observed for Co–LiH.[51,56] In another study, formation of Li–Fe ternary hydride cluster $[Li_4FeH_6]^-$ is a possible active site with reaction mechanism analogous to homogenous coordination

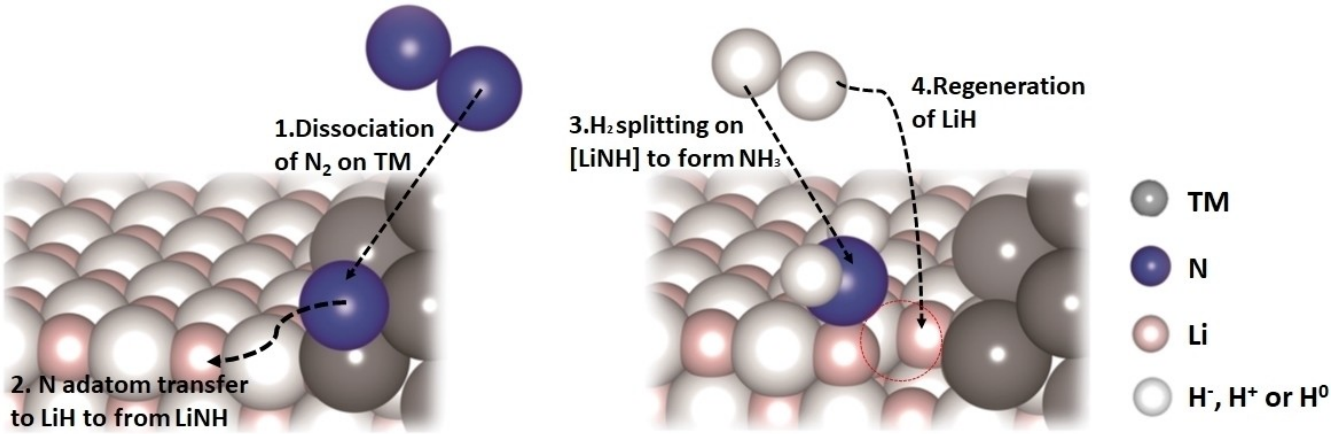

Figure 4. Mechanistic proposal and validation of the two-active-center catalysis in TM-LiH catalysts.[56] Reproduced with permission from Ref. [56] Copyright 2016, Springer Nature.

Table 2. Physicochemical properties and catalytic activity in NH_3 synthesis over the hydride catalysts. (Reaction conditions: Catalyst = 30 mg, N_2:H_2 = 1:3, WHSV of 60,000 ml g^{-1} h^{-}1, *Entry 12–20, Catalyst = 1 g, N_2:H_2: Ar = 22.5:67.5:10, Total flow = 110 ml/min. ** Entry 21: Catalyst = 0.1 g, N_2:H_2 = 1:3, Total Flow = 60 ml/min.)

Entry	Catalyst	Surface Area [m^2/g]	Particle Size [nm]	Temperature [°C]	Pressure [MPa]	NH_3 yield [μmole/g/h]	Ea [kJ/mole]	Ref
1	Fe–LiH	15.7	29.6	300	1	4500	46.5	[56]
2	Mn–LiH	18.7	10.6	300	1	3000	50.6	[56]
3	Co–LiH	42.5	27.6	300	1	4800	52.1	[56]
4	Cr–LiH	–	–	300	1	3500	63.6	[56]
5	Cs–Ru/MgO	–	–	300	1	1200	109	[56]
6	Mn_4N–LiH	16.8	26.1	300	1	2253	–	[57]
7	Mn_4N–BaH_2	6.7	–	300	1	1322	–	[57]
8	Mn_4N–KH	11.8	–	300	1	~500	–	[57]
9	Mn_4N–NaH	18.0	–	300	1	~50	–	[57]
10	Mn_4N–CaH_2	11.4	–	300	1	~400	–	[57]
11	Co–BaH_2/CNT	53	42	300	1	4800	58	[51]
*12	TiH_2	10.5	–	400	5	2800	~75	[59]
13	Cs–Ru (0.9 wt%)/MgO	–	–	400	5	2700	109	[59]
14	$BaTiO_{2.5}H_{0.5}$	15.6	–	400	5	1400	~75	[59]
15	Ru(0.9%)/$BaTiO_3$	–	5.6	400	5	4100	89	[60]
16	Ru(0.9%)/$BaTiO_{2.5}H_{0.5}$	–	6.4	400	5	28800	83	[60]
17	Fe(0.4%)/$BaTiO_3$	–	5	400	5	200	117	[60]
18	Fe(0.4%)/$BaTiO_{2.35}H_{0.65}$	–	5	400	5	1400	63	[60]
19	Co(0.3%)/$BaTiO_3$	–	5	400	5	14	–	[60]
*20	Co(0.3%)/$BaTiO_{2.35}H_{0.65}$	–	5	400	5	550	69	[60]
**21	Ru/$BaCeO_{3-x}N_yH_z$	–	–	400	0.9	30000	–	[22]
22	0.8% Ru/GdHO	–	–	400	5	168000	–	[61]

compounds.[58] The identification of $[Li_4FeH_6]^-$ cluster hints that hydride may also participate in N_2 activation. Still, the confusion exists on H_2/N_2 activation at molecular level for hydrides with two active centers making additional experiments and characterization necessary to draw any further conclusions.[51,58]

Later studies unusually reported TiH_2 as first hydride for NH_3 synthesis without TM/TMN requirement.[59] Studies on TiH_2 confirm that partial surface nitridation is possible during reaction and these nitrides are actual active site for reaction. Strong Ti–N bond suggests the reaction follows the Mars van Krevelen mechanism (direct exchange with lattice N and H species in catalysis). Additionally, high pressure and temperature play a crucial role in nitridation and catalysis. Moreover, TiN, TiO_2, Ti_2O_5 were not active therefore having Ti center and hydride anion together is crucial for critical activity.[59] Low cost TiH_2 exhibited catalytic activity similar to Cs–Ru/MgO, still scope for increasing surface area and activity is in developing stage. (Table 2, Entry 12–13) NH_3 synthesis rate for simple TiH_2 is still lower in comparison to metal hydride mediated Co–LiH and Co–BaH_2 catalysts.[59]

Perovskite hydrides such as Barium oxyhydride ($BaTiO_{2-x}H_x$) were reported to be active in NH_3 synthesis.[59,60] (Table 2, Entry 14) Active species for reaction are oxynitride hydrides ($BaTiO_{2.5}N_{0.2}H_{0.3}$) formed under reaction conditions, hence $BaTiO_3$, $BaTi_{2.5}N_{0.3}$ were inactive. Loading active metals (Ru, Co, Fe) on $BaTiO_{2-x}H_x$ further improved the proficiency of the catalyst. High catalytic activity of metals (Ru, Co, Fe) supported on $BaTiO_{3-x}H_x$ compared to $BaTiO_3$ stipulates hydride sites are indeed essential for catalysis (Table 2, Entry 15–20) Detailed kinetic and isotopic exchange studies show interesting metal dependent support effect i.e $BaTiO_{2-x}H_x$ can act both as hydrogen or electron donor depending on metal present on support.[60] $Ru/BaTiO_3$ and $Ru/BaTiO_{2.5}H_{0.5}$ with comparable N_2 activation energy (~85 kJ/mole) differ largely in H_2 order of reaction, demonstrating low hydrogen poisoning on metal surface by H^- in $BaTiO_{2-x}H_x$. (Figure 5a). The isotopic studies show that lattice hydrides and hydride exchanged N^{3-} take part in reaction through Mars van Krevelen mechanism to form NH_3.[60] But, for $Fe/BaTiO_{2.5}H_{0.5}$ catalyst electrons (instead of hydrides) are transferred from oxyhydride support to Fe particles and cleavage of N≡N is RDS due to very low N_2 reaction order and activation energy (~54 kJ/mol) compared to $Fe/BaTiO_3$ (Figure 5b). Moreover, Ru supported catalysts on series of lanthanum oxyhydrides (LnHO) exhibited superior NH_3 synthesis rate than $BaTiO_{2.5}H_{0.5}$.[61] (Table 2, Entry 22) Such a high activity was due to the pressure induced anion order-disorder transition(H^-/O^{2-}) making the hydride size flexible with easy H^- diffusion during the reaction.

Later work by Hosono group on perovskite oxynitride-hydride catalysts ($Ru/BaCeO_{3-x}N_yH_z$) further confirmed that N–H formation by lattice N^{3-} and H^- is RDS and proceeds along the Mars-Van Krevelen mechanism.[22] $Ru/BaCeO_{3-x}N_yH_z$ exhibited excellent NH_3 synthesis rate compared to other oxyhydrides (Table 2, Entry 21) Novel ABO_3 perovskites (A-alkaline metal, B-lanthanum metals) with wide tuned compositions at A and B sites can potentially be interesting catalysts to investigate in wider range of materials.

Recently, Hosono group developed a novel cubic CaFH solid solution(a kind of hydride), which has ability to form NH_3 at 50 °C with very low activation energy of 20 kJ/mol.[62] This is the first report of any catalyst in NH_3 synthesis at lower temperature and pressure. CaFH catalyst design strategy inspired by their earlier work on CaH_2 electride. Their objective was to modify CaH_2 in way that can reversible exchange hydride even at lower temperature than 200 °C and was achieved by introducing partly F^- anions in to the CaH_2. The F^- anion being hard base compared to H^-(soft base) will strongly bind to the hard acid (Ca^{2+}) though Ca–F ionic bond. This would weaken the bonding between Ca^{2+} and H^-, thereby lowering temperature required for the release of H atoms. At the same time, energy of electrons present in the H^- vacancies increases due to strong repulsion between electron and F^- reducing the work function (2.2 eV) and enhances strong electron donating capabilities to Ru. NH_3 synthesis rate on Ru/CaFH was around 50 and 200 μmole/g/h at 50 and 125 °C at 0.1 MPa.

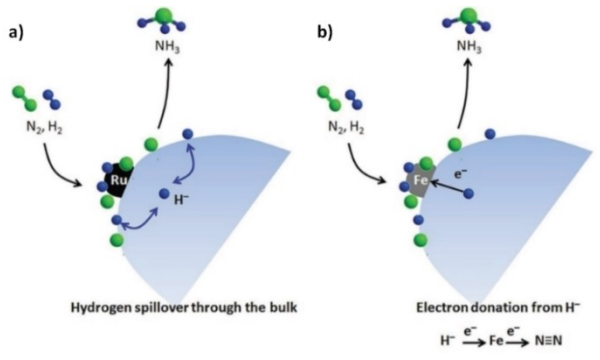

Figure 5. Proposed reaction mechanism for a) $Ru/BaTiO_{3-x}H_x$, proceeds by spillover of H^- through supported particle, b) $Fe/BaTiO_{3-x}H_x$, proceeds by partial donation of electron from H^- to Fe particle thus assisting N_2 activation.[60] Reproduced with permission from Ref. [60] Copyright 2018 WILEY-VCH Verlag GmbH & Co. KGaA, Weinheim.

2.3. Nitrides

In late 20th century, high N_2 adsorption properties of early transition metal predicted nitrides as probable catalysts for NH_3 synthesis.[21,63–67] In this regard, several binary nitrides of Mo, U, V and Re were explored.[58–62] Detailed mechanism of binary nitride in NH_3 synthesis is well documented in review by J Hargreaves.[21,68] Hence, current section is devoted to more recently explored ternary nitrides that are more stable and active compared to binary nitrides in NH_3 synthesis. In 2000, Kojima et al. reported that Cs promoted Co_3Mo_3N produced higher NH_3 rate (986 mole/g/h) compared to doubly promoted Fe catalyst (330 μmole/g/h).[69,70] (Table 3, Entry1-2) In the same year, another research group reported a series of ternary nitrides Co_3Mo_3N, Fe_3Mo_3N and Ni_2MO_3N exhibited similar (~100 ml/h/g) NH_3 synthesis rate at high pressure (50-100 bar), and further addition of Cs promoter abruptly enhanced activity of Co_3Mo_3N, (1040 ml/h/g).[71] High catalytic activity was due to

Table 3. Physiochemical properties and catalytic activity in NH_3 synthesis over nitride catalysts. (Reaction Conditions: Catalyst = 0.4 g, Total Flow = 60 ml/min, $H_2:N_2 = 3:1$.* Catalyst = 0.1 g.)

Entry	Catalyst	Surface Area [m^2/g]	Temperature [°C]	Pressure [Mpa]	NH_3 yield [μmole/g/h]	Ref
1	Co_3Mo_3N	21	400	0.1	652	[70]
2	$Cs_2Co_3Mo_3N$	16	400	0.1	986	[70]
3	Co_3Mo_3C	13	500	0.1	461	[87]
4	Co_3Mo_3N	18	500	0.1	489	[87]
5	Ni_2Mo_3N	8.7	400	0.1	383	[84]
6	$Ni + Ni_2Mo_3N$	6.5	400	0.1	15	[84]
7	Ni_2Mo_3N	2.2	500	0.1	272	[91]
8	$CoNiMo_3N$	8.0	400	0.1	160	[84]
9	$Ni_{1.7}Cu_{0.2}Mo_3N$	1.8	500	0.1	231	[91]
10	$Ni_{1.1}Fe_{0.9}Mo_3N$	2.8	500	0.1	354	[91]
11*	Ni(12.5 %)/LaN(Nanoparticles)	42.6	400	0.1	5543	[94]
12	LaN–Ru(2 wt%)/ZrH_2	2.0	350	1.0	305000	[95]

good atomic mixing of metals in Co_3Mo_3N and alkali promoter (Cs) acting as inhibitor for NH_3 poisoning on Co_3Mo_3N.[70,72,73]

Meanwhile, theoretical investigation showed that a volcano shaped relation exists between the NH_3 synthesis over different metal catalysts and their N_2 adsorption energy as show in Figure 6.a.[74] Volcano plot concluded Co–Mo alloy, combining metals with very low (Co) and high (Mo) adsorption energy for N_2 will provide an optimum N_2 adsorption energy sufficient to activate N_2 molecule.[74,75] Hence, Co_3Mo_3N displayed higher TOF than their constitutional Co and Mo metal.[74] Studies demonstrate that, (111) surface of CoMo alloy exists in the form of Co–Mo–N structure during reaction conditions. Hence, role of lattice N in Co_3Mo_3N is crucial for catalytic activity. For long time, the role of lattice N species in nitride catalyst was debated with RDS as direct N_2 activation or hydrogenation of bulk (lattice) N.[21] Initial, adsorption experiments reveal that lattice nitrogen of ternary nitride does not participate in reaction but is necessary for good atomic mixing of Co and Mo to form an ordered Co–Mo surface.[74] In contrary, study via temperature programmed reaction of Co_3Mo_3N with Ar/H_2 and benzene produced Co_6Mo_6N and Co_3Mo_3C respectively, indicating lattice N are reactive and are mobile. Further, heating Co_6Mo_6N in presence of H_2/N_2 or N_2 regenerates back to Co_3Mo_3N.[76,77] Hence, Co_3Mo_3N acts as active nitrogen reservoir that can be released and restored by changing the gas feed (Ar/H_2 or N_2/H_2).[78] Out of 50 % lost lattice nitrogen, around 20 % of lattice N in Co_3Mo_3N are involved in formation of NH_3.[77,79] Nevertheless, formation of NH_3 through loss of lattice N as N_2 (then dissociation of N_2) or by direct hydrogenation of lattice N to form NH_x was unclear.[78] To understand this unknown phenomenon Hunter et al. carried out the nitrogen isotopic exchange reaction.[80] The atomic fraction of $^{15}N_2$ in the gas phase decreased after Co_3Mo_3N scrambled with mixture of $^{14}N_2$ and $^{15}N_2$, suggesting that a heterolytic exchange between gas phase species and lattice N is possible. These results demonstrate the possibility of a Mars-van Krevelen mechanism, hydrogenation of lattice N, and latter lattice vacancies being refilled from gas phase N_2. Further, semi empirical calculations show 3 fold hollow bound nitrogen containing (111) surfaces have higher amount of N vacancies in temperature range of NH_3 synthesis and can adsorb and activate N_2 and H_2.[80,81] The DFT study suggests H_2 can adsorb on MoN_3 framework and undergo dissociation on Co_8 clusters or N vacancies.[82] (Figure 6. b) The N_2 with three possible different adsorption configurations over

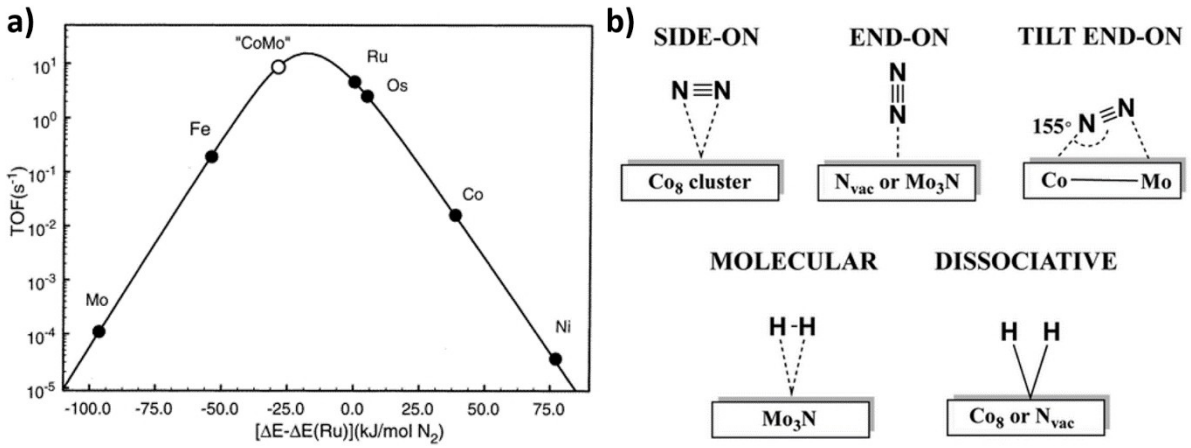

Figure 6. a) Calculated turnover frequencies for NH_3 synthesis as a function of the adsorption energy of nitrogen,[74] Reproduced with permission from Ref. [74] Copyright 2001 American Chemical Society. **b)** Simplified schematic showing different adsorption configurations of N_2 and H_2 over different active sites in Co_3Mo_3N.[80] Reproduced with permission from Ref. [80] Copyright 2013 American Chemical Society.

different sites is more likely to be activated by inner tetrahedral atom of Co_8 cluster with side-on configuration. (Figure 6. b) Apart from the Langmuir Hinshelwood and Mars van Krevelen mechanism, another distinct mechanism is proposed, where hydrogen reacts directly with surface activated N_2 to form hydrazine and diazane intermediate in order to produce NH_3, and is likely to follow Eley-Rideal mechanism.[83] Overall, participation of lattice N was realized with different mechanism route possible over Co_3Mo_3N in NH_3 synthesis.

Since, lattice N plays crucial role in N_2 activation, synthesis method adopted for ternary nitrides such as nitridation environment, use of oxide precursor, and presence of impurity, affects NH_3 synthesis rate considerably.[84,85] Nitridation of Co–Mo oxides by ammonolysis (treating with NH_3) generates superior quality Co_3Mo_3N, than treating with N_2/H_2, but latter is more easily manageable at industrial scale.[84] In another work, Co_3Mo_3N nanoparticles supported on CeO_2 exhibited 20 times higher activity than bulk Co_3Mo_3N.[86] Reports also demonstrate that not only oxides, but carbides can also be precursor for synthesis of nitrides. Co_3Mo_3C in presence of reactant gas mixture (N_2+H_2) at 400 °C undergoes nitridation to form Co_3Mo_3N and exhibits catalytic activity similar to the pure Co_3Mo_3N.[87] (Table 3, Entry 3–4) Unlike Co_3Mo_3C, for Fe_3Mo_3C, NH_3 synthesis was possible at high temperature of 500 °C with formation of Fe_3Mo_3N. Unfortunately Ni_2Mo_3C could partially replace the lattice carbon by nitrogen to form $Ni_2Mo_3C_xN_y$.[88] But such carbo-nitrides are not active in NH_3 synthesis.[89] Hence, chemical composition, temperature and pre-treatment conditions are crucial for synthesis of high quality nitrides from their oxides or carbide precursor.

Ni_2Mo_3N(2-3-1) with different compositions than Co_3Mo_3N(3-3-1) attracted interest for NH_3 synthesis. Still it is unclear on the formation of Ni_2Mo_3N instead Ni_3Mo_3N.[90] Ni_2Mo_3N synthesized from $NiMoO_4$ exhibited Ni impurity along with Ni_2Mo_3N, but Pechini method with use of citrate gel resulted in pure Ni_2Mo_3N without any Ni impurity that exhibited higher NH_3 synthesis rate than the former catalyst.[84] (Table 3, Entry 5–6) Unlike Co_3Mo_3N (η-6 carbide structure), Ni_2Mo_3N crystallizes in β-Mn structure with low extent of lattice N exchange, hence lower activity in comparison to Co_3Mo_3N.[84] Additionally, partial substitution Co, Cu and Fe at the nickel sites in Ni_2Mo_3N has no major influence on the electronic properties hence no enhancement in NH_3 synthesis rate.[91] (Table 3, Entry 7–10) Preliminary studies reported antiperovskite nitrides (Co_3ZnN, Ni_3ZnN, Co_3InN, and Ni_3InN) can produce NH_3 in H_2/Ar atmosphere. Lattice N of these compounds are converted to into NH_3, but further regeneration of lattice N was not realized and advanced research is necessary to efficiently produce NH_3 with long life.[92] $CoRe_4$ alloy with *in situ* formed nitride during reaction was active for NH_3 synthesis but use of costly Re makes it less attractive industrially.[93]

Recent contemporary studies on Ni loaded lanthanum nitride (LaN) and LaN promoted Ru/ZrH_2 catalyst disclosed nitrides with surface nitrogen vacancies can efficiently activate the N_2.[94,95] The NH_3 synthesis on Ni/LaN catalyst occur though dual site mechanism that evades commonly challenged scaling factors. Kinetic, isotope labelling and DFT studies confirm the formation of N vacancies at surface with small formation energy, efficiently bind, and activate N_2. In addition, H_2 dissociation occurs on Ni site and Ru/ZrH_2. Synergy between these sites activates both the reactants. Both catalyst exhibits activity that exceeds the conventional Cobalt and Nickel catalyst, and are comparable to the Ruthenium based catalysts. (Table.3 Entry 11–12)

2.4. Intermetallic/Alloy

Intermetallic: Currently, intermetallic compounds (IMCs) with their unique ordered structural and electronic properties driven more curiosity in heterogeneous catalysis.[96–100] The IMCs described earlier in section 2.1 are involved in NH_3 synthesis through their electride properties. However, catalytic activity also be attained without electride properties due to their structural and ligand effects. There has been limited IM/alloy compounds that studied for the NH_3 synthesis long back in 19th century.[53,101] The rare earth IMC of Ce with other metals like Co, Ru, and Fe exhibited good activity compared to respective metals. However, post-catalytic characterization disclosed the decomposition of IMC to the rare earth metal nitride and transition metal (Fe).[53,101] The reason for the decomposition is still not clear. With quite a few attempts made, it appears that alloying induces less drastic effect on NH_3 synthesis reaction.[102,103] Recently Hosono group reported, Ru_2Y, laves phase of IMC with excellent hydrogen storage enhances N_2 activation by increasing electron density on Ru connected to Y in the structure.[104] (Table 3, Entry 11) Synthesis of Ru_2Y with high surface area by laser ablation technique overcomes application of bulk IMCs as catalysts.[104] Ru_2Y synthesized by laser ablation with surface are of 6.4 m^2/g exhibited activity 3318 μmoles/g/h, 10 fold greater compared to bulk Ru_2Y at 400 °C and 0.1 MPa. Ru_2Y with special electronic and geometrical structures is another example demonstrating Ru with absence of B_5 site could catalyze NH_3 synthesis.[104] In another study $RhCo_3/CoO(011)$ was predicted to catalyze NH_3 synthesis analogues to biologic process where hydrogenation of N_2 occurs with activation of N_2 on both metal sites.[105]

Alloy: Unlike IMCs, alloys have disordered structures and very few catalysts have studied for NH_3 synthesis. Ru–Fe supported on MgO exhibited higher activity than Ru/MgO and Fe/MgO with resistance to N and H poisoning at high pressure.[106] Several theoretical studies suggest alloying Ru with other metals (Pt, Rh) will improve the B_5 site necessary for efficient N_2 activation.[107] Goddard et al. predicted that Rh doping with Fe would increase the TOF for NH_3 synthesis by a factor of 3 compared to Fe (111).[108] Doping Rh with other elements such as Pt, Cu, Pd may also dramatically improve the TOF compared to Rh.[107,108]

2.5. Oxides

Lanthanum oxides: In addition to acting as promoter lanthanum oxides are also potential supports in NH_3 synthesis. In

earlier studies by Aika et al. on Lanthanum based oxides ($CeO_2.Sm_2O_3$, La_2O_3) show that they are good catalyst supports with high catalyst density.[109] Recent development on Ruthenium supported CeO_2 and Pr_2O_3 gave broader view on the role of support metal interactions. CeO_2 with Ce^{+4}/Ce^{3+} redox ability and oxygen vacancies increases electron density on Ru, hence is an excellent support for NH_3 synthesis.

Ma et al. reported the effect of difference morphology of CeO_2 on NH_3 synthesis. Studies show that concentration of oxygen vacancies is dependent on the morphology of the CeO_2 particles.[110] Rods(R), spherical(S) and cubic(C) shaped CeO_2 particles with (110), (111) and (100) exposing planes having similar size (100-300 nm) were synthesized by hydrothermal method. (Figure 7.b–d) The concentration of oxygen vacancies was related to the Ce^{3+}/Ce^{4+} ratio and are in the following order : Ru/R–CeO_2(0.59) > Ru/C–CeO_2(0.46) > Ru/S–CeO_2(0.32). R–CeO_2 possesses high oxygen vacancies and Ru dispersion, and very low activation energy (108 kJ/mole) compared to S–CeO_2(132 kJ/mole) and C–CeO_2 (124 kJ/mole). XPS and Raman spectroscopies confirm strong support metal electronic interaction with formation of Ru–O–Ce and Ru^{n+} species through which electrons transfer is efficient for activation of N_2. (Figure 7.a) Later, Lin et al. also observed high catalytic activity for Ru/R–CeO_2 compared to Ru/C–CeO_2.[111] In contrary to Ma et al studies, Lin et al., observed similar Ce^{3+}/Ce^{4+} ratio of ~0.20 for both Ru/C–CeO_2 and Ru/R–CeO_2, concluding decisive factors in the formation of oxygen vacancies is not Ce^{3+}/Ce^{4+} but particle size and chemical state of Ru species.[111] The Ru species in R–CeO_2 catalyst are merely crystalline and are majorly in oxide state (Ru^{n+}), while Ru particles in C–CeO_2 catalyst are metallic (Ru^0) in nature with large particle size. Presence of such Ru–O species on Ru/R–CeO_2-rod is beneficial for H_2 adsorption through formation of hydroxyl group, while oxygen vacancies enhance the N_2 adsorption and enhance NH_3 formation as seen from Figure 7.e.[111] Hence, these hydroxyl group act similar to hydrides as observed in electrides earlier. Such hydroxyl group formation is not possible on metallic Ru^0 in Ru/C–CeO_2 as results lower oxygen vacancies and most of hydrogen species consumed in H_2O formation. The NH_3 synthesis rate vs time on stream studies show that CeO_2 with rod morphology is better in NH_3 synthesis rate (3700 μmol/g/h), additionally Cs, K and Ba promoter improved NH_3 synthesis rate (Table 4, Entry 1–6)

Concentration of oxygen vacancies at the surface of CeO_2 can also be varied using different precipitation agents during synthesis. Li et al. hydrothermally synthesized CeO_2 using 3 different precipitating agents : mainly, Tetra propyl ammonium hydroxide (TPAOH), ethylene diamine (EDA) and NaOH. Ru/CeO_2-TPAOH with high concentration of oxygen vacancies exhibited superior catalytic activity than Ru/CeO_2-EDA and Ru/CeO_2–NaOH.[112] (Table 3, Entry 7–10)

Numerous reports were also focused on enriching the oxygen vacancies in CeO_2 by introducing metal such as La, Zr, Ti.[113–116] Sato et al. developed La doped ceria ($La_{0.5}Ce_{0.5}O_{1.64}$) support as an effective support compared to CeO_2 and La_2O_3.[117] Doping of La, improved stability of Ru/CeO_2 above 550 °C and increased oxygen vacancies at surface through partial reduction of support. The EEL studies revealed that fine Ru nanoparticles of size 1.8 nm are partially covered on all sides by reduced support through strong SMSI, except from top (accessible for reactants) as seen from the Figure 8. a. As a result, electron transfer from reduced support to the Ru metal greatly enhanced and electrons transferred to N_2 for activation (direct interaction). Ru/$La_{0.5}Ce_{0.5}O_{1.64}$ catalyst reduced at 650 °C with very low activation energy of 64 kJ/mole exhibited high NH_3 synthesis rate of 31.3 mmol/g/h compared to Ru/CeO_2 and Ru/La_2O_3.[117] (Table 3, Entry 10–13) Further addition of Ba promoter, covered Ru nanoparticles creating composite oxide "nano fractions", including Ba, Ce^{3+} and La^{3+}.[118] (Figure 8b) Such low crystalline and oxygen deficient compounds of oxides (nanofraction) accumulated on the Ru nanoparticle have strong

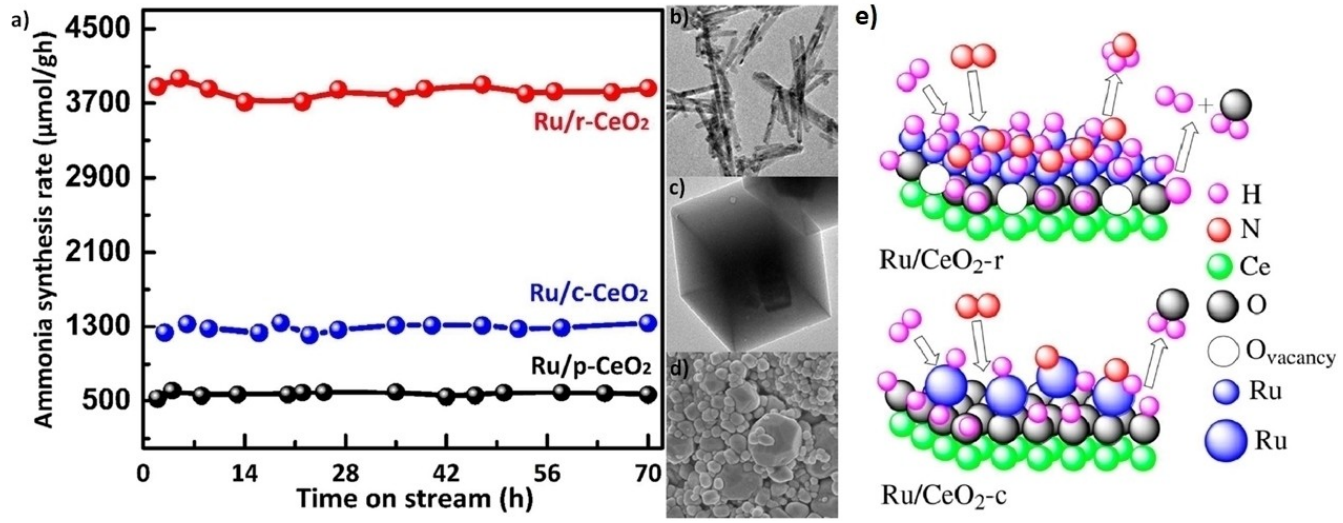

Figure 7. a) Morphology effect of CeO_2 on the catalytic performance of Ru/CeO_2 in NH_3 synthesis and TEM Images of **b)** rod **c)** cubic and **d)** spherical CeO_2 particles.[110] Reproduced with permission from Ref. [110] Copyright 2017 Royal Society of Chemistry. **e)** Proposed reaction pathway for the formation of Hydroxyl, hydrogen, water and NH_3 on the Ru/CeO_2 catalyst.[111] Reproduced with permission from Ref. [111] Copyright 2018 American Chemical Society.

Table 4. Physiochemical properties and catalytic activity in NH_3 synthesis over Lanthanum oxide supported catalysts. (Reaction Conditions: Catalyst = 0.2 g, H_2:N_2 = 3:1, Total Flow = 60 ml. * catalyst = 150 mg, WHSV = 24000. **Catalyst = 100 mg, Total flow rate = 120 mL min^{-1} # GHSV of 70,000 h^{-1}, catalyst = 0.2 g.)

Entry	Catalyst	Ru Loading [wt%]	Surface Area [m^2/g]	Particle Size [nm]	Temperature [°C]	Pressure [Mpa]	NH_3 yield [μmole/g/h]	Ea [kJ/mole]	Ref
1	Ru/rod–CeO_2	4	63.7	–	400	1	3830	108	[110]
2	Ru/cubic–CeO_2	4	58.4	–	400	1	1289	124	[110]
3	Ru/spherical–CeO_2	4	31.2	–	400	1	529	132	[110]
4	2Cs_Ru/rod–CeO_2	4	–	–	400	1	14266	–	[110]
5	2Ba_Ru/rod–CeO_2	4	–	–	400	1	6638	–	[110]
6	2 K_Ru/rod–CeO_2	4	–	–	400	1	11227	–	[110]
7*	Ru/CeO_2–TPAOH	2.5			450	3	22000		[112]
8*	Ru/CeO_2–EDA	2.5			450	3	19000		[112]
9*	Ru/CeO_2–NaOH	2.5			450	3	16500		[112]
10*	4%Cs, Ru/CeO_2–TPAOH	2.5			450	3	32000		[112]
11**	Ru/$La_{0.5}Ce_{0.5}O_{1.64}$ −650 C	5	42	1.7	350	1	31300	64	[117]
12**	Ru/CeO_2 −650	5			350	1	17200		[117]
13**	Ru/La_2O_3 −650	5			350	1	10800		[117]
14**	Ba/Ru/$La_{0.5}Ce_{0.5}O_{1.64}$ −700	5	21	2.45	350	1	52300	67.2	[118]
15*	Ru/Pr_2O_3	5	20.4		400	1	19000		[119]
16**	Ru/$La_{0.5}Pr_{0.5}O_{1.64}$ −650 C	5	30	2.9	400	1	60200		[121]
17	Ru/$Ti_xCe_{1-x}O_2$	3	–	–	400	1	10861		[114]
18	Ru/$Zr_{0.4}Ce_{0.6}O_2$	4	–	–	390	1	1700	93	[113]
19#	Co/CeO_2-dopamine	–	–	–	425	1	19200		[122]
20#	Co/CeO_2	–	–	–	425	1	3810		[122]

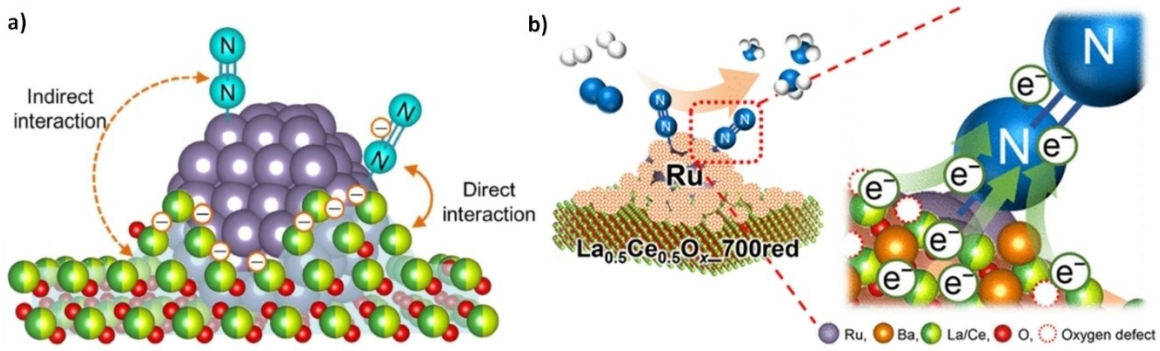

Figure 8. a) Possible mechanism for the activation of N_2 over Ru/$La_{0.5}Ce_{0.5}O_{1.64}$, direct interaction between N_2 and reduced oxide partially surrounded Ru nanoparticle is possible.[117] Reproduced with permission from Ref. [117] Copyright 2018 Royal Society of Chemistry. **b)** Possible mechanism of N_2 activation on a surface available Ru atom in contact with the reduced nanofraction oxide in Ba promoted Ru/$La_{0.5}Ce_{0.5}O_{1.64}$ catalyst.[118] Reproduced d with permission from Ref. [118] Copyright 2020 American Chemical Society.

electron donating ability, improves the NH_3 synthesis rate to 52.3 mmol/g/h. (Table 3, Entry 14) However, Ba promoted Ru/$La_{0.5}Ce_{0.5}O_{1.64}$ exhibits high activation energy compared to unprompted Ru/$La_{0.5}Ce_{0.5}O_{1.64}$ indicating blockage of some of Ru active sites by nanofraction for the reactants. Ru/$La_{0.5}Ce_{0.5}O_{1.64}$ exhibited highest NH_3 synthesis rate among oxide-supported catalysts reported so far in literature.

Similar to CeO_2, low crystalline Ru nanolayer supported Pr_2O_3 exhibited excellent NH_3 synthesis rate and was further enhanced by La doping.[119–121] (Table 3, Entry 15–16) Substitution of metals such as La, Zr and Ti in CeO_2 helps in formation of oxygen vacancies that eventually improve electron donation to Ru and enhances catalytic activity.[113–116] (Table 3, Entry 17–18) Not only Ru, CeO_2 support can stabilize and activate Co nanoparticles for N_2 activation.[122] Use of dopamine as anchoring agent could improve substantially SMSI between Co and CeO_2.[122] (Table 3, Entry 19)

Perovskites: Perovskite with ABO_3 structure have been widely studied as support for both electro and thermochemical NH_3 synthesis owing to their high thermal stability, proton conductivity, redox properties and ready availability.[123] The electronic properties can be tuned by varying both A and B sites, as more precisely catalytic activity depends on both sites. Additionally A sites are also responsible for stabilizing perovskite structure.[124] In 2010, Yang et al. first reported Ru loaded $BaCeO_3$ as catalyst for NH_3 synthesis, subsequently Ru/$BaZrO_3$, Ru/$BaTiO_3$ were investigated.[124,125] With decrease in electronegativity of metal at A in these catalysts increased NH_3 synthesis rate in the following order Ru/$CaTiO_3$ < Ru/$SrTiO_3$ < Ru/$BaTiO_3$.[124] (Table 4, Entry 1–3) The alkaline-earth elements (A site) provide promotional effects on catalytic activities of Ru nanoparticles through their basicity. Ru/$BaTiO_3$ with comparable activity to Ba–Ru/MgO and Cs–Ru/MgO, exhibited good stability for 24 h, while Ru/MgO deactivates at 18 h. Among different

metals varied at B sites in $BaBO_3$, NH_3 synthesis rate decreased in the following trend: $BaZrO_3 > BaCeO_3 > BaTiO_3$.[126,127] (Table 4, Entry 4–7) Further adding Cs promoter to $Ru/BaZrO_3$enhances the NH_3 synthesis rate.[128] (Table 4, Entry 8) Exact electronic or geometrical influence of metal present at B site on N_2 dissociation or Ru dispersion is unclear and would require systematic examination. But partial substitution of Y^{3+} in B Site (Zr and Ce) of perovskite shows significant improvement in NH_3 synthesis due to the formation of oxygen vacancies and SMSI.[129]

In another interesting study, Jiang et. al, incorporated small amount of (> 1 wt%) Ru into Co/Zr sites of $LaCoO_3$ and $LaZrO_3$ structure, enhancing number of active sites and SMSI. $LaCoRu_{0.02}O_3$ exhibited activity superior than $LaCoO_3$and $Ru/LaCoO_3$.[130,131] (Table 4, Entry 9–12) However, use of $RuCl_3$ precursor for synthesis of $Ru/LaCoO_3$ is inadequate for its comparison with $LaCoRu_{0.02}O_3$ due to the Cl^- poisoning. Strontium niobate with perovskite like structure induces epitaxial growth of truncated pyramid shaped Ru nano crystallites with abundant steps and B_5 sites displaying NH_3 synthesis better than Cs–Ru/MgO.[132] (Table 4, Entry 13) These studies indicated that, perovskites look to be promising supports for Ru in NH_3 synthesis and require fine-tuning extensive studies devoted to further understand the catalytic mechanism.

2.6. Carbon support

Commercialization of Ru/Activated Carbon catalysts in industry demonstrates that they are more promising than oxide supported catalysts due to their unique electronic properties.[136] Carbons supports such as carbon nanotubes,[137] activated carbon (AC),[138–141] mesoporous carbon (MC),[142] and graphitic nitrides (GN).[143,144] were widely studied for NH_3 synthesis. Carbon materials are potentially excellent supports due to the uniform dispersion of Ru nanoparticle, but activity extremely dependent on synthesis strategy, porosity, surface area and surface functional groups.[145–147] The major disadvantage with carbon support is methanation of carbon occurring at NH_3 reaction conditions, as result metal sintering and loss of active components occur with declined catalytic activity.[148] However, this was overcome by doping, functionalization of carbon support along with addition of alkali/alkaline metal as promoter. Initial studies have shown Ba and K promoters with oxygen rich functional groups present on AC has improved Ru dispersion, stability and catalytic activity in NH_3 synthesis.[149–151] Recently Jiang et al. have reported that addition of La to Ba–K–Ru/AC has inhibited methanation of carbon.[152] The strong interaction of reduced LaOx layer beneath Ru particles has suppressed contact between carbon support and Ru particles as result inhibited formation of H species necessary for methanation.[152] Nevertheless, conventional carbon supports with lower pore size (< 2 nm) encounter diffusion limitations and lower dispersion of Ru nanoparticles.

To improve catalytic performance, mesoporous carbon (MC) with high surface area and tunable pore diameters with nano-sized support were adopted for NH_3 synthesis. Cs, Ba, promoted MC catalysts displayed high dispersion for (46%) Ru nanoparticles with uniform size of 2 nm (Cs–Ru/MC) exhibiting high NH_3 synthesis rate 8–10 mmol/g/h compared to Cs–Ru/AC (3.45 mmol/g/h).[142,153] BaO_x and CsOH promoter adhered to the Ru nanoparticles improved the B_5 sites and enhanced electron density on Ru for the activation of N_2. The Cs–Ru/MC exhibited excellent response and stability during recycling tests over severe temperature jumps in a short time due to the mesoporous carbon framework and promoter.[142,154] Li et.al., synthesized, Ru nano particle of size 1.5-2.5 nm, semi embedded in mesoporous carbon (Ba–K/Ru–MC) by novel $RuCl_3/SiO_2$ template approach with Ba/K promoter exhibiting higher catalytic activity than just supported catalyst Ba/K/Ru/MC. Further, incorporation of N in carbon matrix greatly improves catalytic activity of Ba/Ru–N-MC due to SMSI and change in the electronic properties of metallic Ru.[155] Instead of loading, embedding Ru nanoclusters in carbon matrix is more advantageous, as it improves SMSI, stability and avoids sintering.[156] MC composite Sibunit and MOF (Ru-HKUST-1) derived graphitic carbon also work as excellent supports for the dispersion of Ru Nanoparticles with enhanced N_2 activation.[157,158]

In another study, an interesting carbon coated Al_2O_3 composite was developed by Jiang et. al for NH_3 synthesis.[159] Al_2O_3 coated with carbon using two different methods such as sucrose pyrolysis and acetylene decomposition. Carbon with more hydroxyl groups were obtained by sucrose pyrolysis than with acetylene decomposition. The presence of –OH groups on carbon enhanced the formation of H_2O and reduced the number of active H adatoms formed on the Ru nanoparticle as result hindering the NH_3 synthesis. This competitive reaction between water evolution and NH_3 synthesis is key factor in controlling activity. Ba–Ru/C–Al_2O_3 (obtained by acetylene decomposition) shows outstanding performance with large amount and low hydration of surface hydrogen, relatively easy desorption of surface N species and more available Ru^0 species. (Figure 9)

2.7. Novel and other Supports

Calcium amide [$Ca(NH_2)_2$] an ionic compound with anatase structure consisting of Ca^{2+} and NH_2^- ions was reported as superior support for Ru nanoparticles in NH_3 synthesis. $Ca(NH_2)_2$ (CA) is not stable above 70 °C, hence decomposes to NH_3 and CaNH.[133] But supporting Ru nanoparticles stabilize CA without decomposing at high temperature as 400 °C and displays high catalytic activity in NH_3 synthesis for long time (45 h). Nitrogen labelled mass spectrometry experiment suggests NH_3 synthesized is not from decomposition of CA but through gaseous N_2 and H_2 over Ru catalyst. High TOF for $Ru/Ca(NH_2)_2$ compared to Cs–Ru/MgO is attributed to the strong electron donation from $Ca(NH_2)_2$ support to Ru.(Table 5, Entry 14) Presence of Ru–N bonds suggesting that Ru atoms are strongly bonded to N atoms of the support. These strong interactions prevent aggregation of Ru particles with formation of 2-dimensional flat Ru nanoparticles rather than conventional particles with

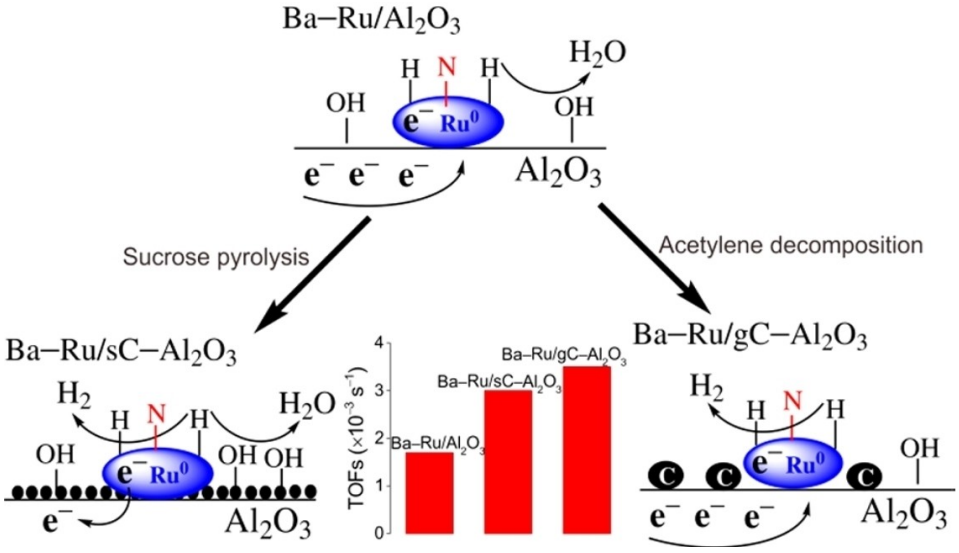

Figure 9. Proposed mechanism for the effect of carbon surface (–OH groups) on hydrogen desorption and NH_3 synthesis.[159] Reproduced with permission from Ref. [159] Copyright 2019 American Chemical Society.

Table 5. Physiochemical properties and catalytic activity in NH_3 synthesis over the Perovskite and novel supported catalysts. (Reaction Conditions: Catalyst = 0.1 g, $H_2/N_2 = 3$; Total flow 60 ml/min, * Catalyst = 0.3 g, **Catalyst = 0.2 g, catalyst = 0.1 g.)

Entry	Catalyst	Ru Loading [wt%]	Surface Area [m^2/g]	Temperature [°C]	Pressure [Mpa]	NH_3 yield [μmole/g/h]	TOF [s^{-1}]	Ref
1	$Ru/CaTiO_3$	2	1.6	400	0.1	268	3.76	[124]
2	$Ru/SrTiO_3$	2	4.6	400	0.1	774	10.8	[124]
3	$Ru/BaTiO_3$	2	3.9	400	0.1	1647	23.2	[124]
4	Ba–Ru–MgO	2	7.8	400	0.1	1919	27.0	[126]
5	Cs–Ru–MgO	2	16	400	0.1	1925	27.0	[126]
6	$Ru/BaZrO_3$	2	15	400	0.1	3630	77	[126]
7	$Ru/BaCeO_3$	2	4	400	0.1	2310	287	[128]
8	4%Cs/Ru/$BaCeO_3$	1.25	–	450	3	28000	–	[128]
9*	$LaCoRu_{0.01}O_3$	0.54	3	450	1	8500	–	[131]
10*	$LaCoO_3$	–	5	450	1	4600	–	[131]
11*	$Ru/LaCoO_3$	0.56	17	450	1	4900	–	[131]
12	$LaZr_{0.95}Ru_{0.05}O_3$	–	–	400	1	5500	–	[130]
13	Cs–Ru/$Sr_2Nb_2O_7$	2	–	400	1	4986	–	[132]
	Novel supports							
14**	$Ru/Ca(NH_2)_2$	10	60	300	0.1	15800	–	[133]
15**	Ba/Ru/SAs/S_{-1}	0.36	–	400	0.1	1400	–	[134]
16#	$Ru/CaCN_2$	5	6.8	300	1	3785	7.3	[135]
17#	$Ru/Ca_2N{:}e^{<c->}$	5	5.3	300	1	1740	5.0	[135]
18#	Ru–Cs/MgO	5	23.6	300	1	553	0.6	[135]

spherical morphology. HAADF-STEM suggested the existence of flat Ru particles due to epitaxial growth of Ru nanoparticles on a support having similar lattice fringes. (Figure 10a) Because of Ru–CA epitaxial adhesion, flat Ru nanoparticles are crystallized in metastable fcc structure than more typically observed hcp structure. Such flat fcc Ru nanoparticles are known to increase high-density B5 sites and promote catalytic performance and long-term stability. NH_3 synthesis mechanism is analogous to that proposed for $Ru/C12A7{:}e^-$ and $Ru/Ca_2N{:}e^-$ systems with N–H formation as RDS. Ba doping distinctly improves stability (700 h) and activity of $Ru/Ca(NH_2)_2$ due to Ru–Ba core shell and mesoporous structure. The added Ba present in the form of $Ba(NH_2)_2$ has low work function with higher electron donation capability than $Ca(NH_2)_2$ promoting more efficient N_2 activation[160] (Figure 10b)

Since, Ca based supports were promising for their superior electron donation to Ru nanoparticles, research in this path is broadening, recently a novel air stable calcium cyanamide ($CaCN_2$) was discovered as excellent support for Ru in NH_3 synthesis.[135] Kinetic investigation shown the low activation energy and high resistance to hydrogen poisoning for $Ru/CaCN_2$ similar to observed for Ru supported electride catalyst. The systematic experimental and theoretical investigation revealed the formation of CN_2 vacancies on the surface of $CaCN_2$ with quasi electride structure, which can store and release H^- during the reaction. The catalytic activity of Ru/

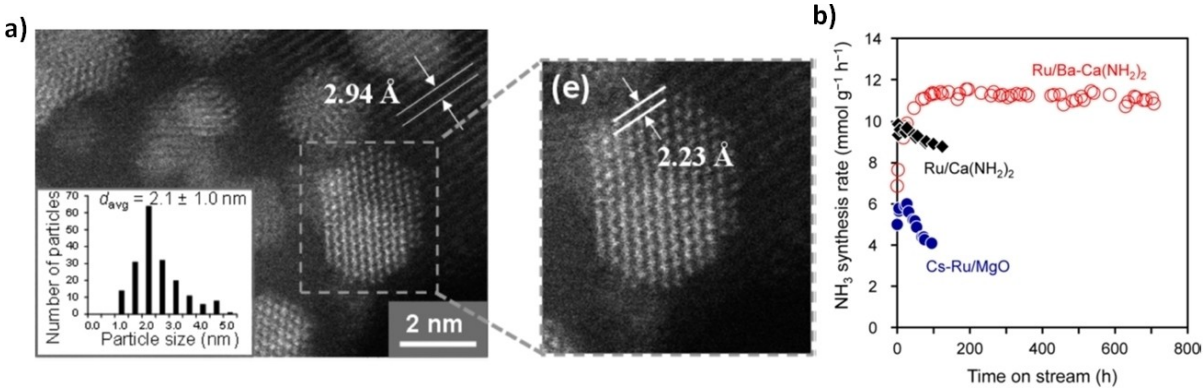

Figure 10. a) HAADF-STEM image of 10 wt % $Ru/Ca(NH_2)_2$ catalyst after NH_3 synthesis showing the flat Ru particles with d spacing related FCC structure, **b)** Time course of NH_3 synthesis on $Ru/Ba–Ca(NH_2)_2$, $Ru/Ca(NH_2)_2$, and Cs–Ru/MgO.[133] Reproduced with permission from Ref. [133] Copyright 2016 American Chemical Society.

$CaCN_2$ was better than the $Ca_2N:e^-$ and Ru–Cs/MgO catalysts. (Table 5, Entry 16–18)

Zeolites are another class of excellent catalysts and supports applied in petroleum refining industries but are scarcely explored in NH_3 synthesis due to their acidic nature.[161] The replacement of acid sites of X and Y zeolite by alkali and alkaline earth metals enhances the basicity in zeolite, but are still less attractive due to weak metal support interaction and rigid Si–O–Al framework that are not capable to enhance electron density on Ru nanoparticle for competent N_2 activation.[162–164] Recently, Jian et al. has reported that pure siliceous zeolite supported Ru single atom active sites are efficient for NH_3 synthesis.[134] Single atom catalysts are always advantageous due to isolated individual atoms dispersed on, and/or coordinated with, surface atoms of appropriate supports, maximizing the atomic efficiency of metals. Use of special Ru-ethylenimine chloride precursor could confine Ru (0.27 % wt %) within SAs/S-1(MFI type) zeolite. The electron microscopy and XPS indicated the absence of any nanoparticle formation indicating Ru is part of zeolite framework with +4-oxidation state. DFT studies shows activation of N_2 occurs through linear adsorption of N_2 on the single Ru sites. The NH_3 synthesis rate of Ru SAs/S-1 was very low (6 μmole/g/h) but was sharply enhanced to 1389 μmole/g/h by high Ba loading(9 wt%) indicating the zeolite support has very low electron interaction with Ru but was widely boosted by Ba promoter.[134] (Table 5, Entry 15) Time dependence of the catalytic activities of Ru SAs/S-1 and Cs–Ru MgO indicates the high stability of the former catalyst than the later. However, for commercial applications, requires incorporating more Ru sites into zeolites and is still challenging. Studies also reveal that some of zeolites FER and MFI could act as potential catalyst for NH_3 synthesis at high pressure (200 bar) and temperature (500 °C).[165]

3. Summary and outlook

Increasing global population, energy cost and demand for NH_3 has motivated continued research for development of more efficient catalyst technologies.[4] Though Fe based and recently commercialized promoted Ru/C catalyst exhibit superior performance, still there is a need for further improvement of catalysts under mild conditions particularly at low temperature and pressure.[136] Major research work devoted before 2010, primarily focused on promoted metal oxides and carbon supported Ru catalysts, and ternary nitrides were at initial stage of development with very less knowledge.[16,66] Lately, advanced innovative supports and active catalysts designed for NH_3 synthesis and deep investigation of these materials have rehabilitated NH_3 synthesis in new direction.[24] Electrides, hydrides, nitrides and oxides with their promising unique properties of reversible electron, hydride, nitride and oxide vacancies storage have tremendously improved Ru based catalysts efficiency. Enormous maturation of experimental and theoretical methods with improved precession over worldwide research effort helped in gaining a fundamental understanding of new materials in NH_3 synthesis.

The major breakthrough studies on $Ru/Ca12A7:e^-$ reveal the N–H formation is RDS and not N_2 activation.[24] Insight gained with reversible hydride storage that inhibited Ru poisoning by H_2 at high pressure in $Ru/Ca12A7:e^-$, captured attention of alternative electrides with more superior hydride storage properties, boosted advanced studies on series of electrides and hydride materials for NH_3 synthesis.[38,46] Electrides with their excellent reversible hydride storage capacity at mild conditions, have drawn attention in the field of rechargeable metal hydride batteries.[166] There are quite a few class of IM hydrides AB_2-Laves phase, AB_5-Hauck phase, (A = rare earth and B = d-and p-block elements) which store hydrogen at moderate temperature and pressure and are essential to be considered.[55,167] Harsh synthesis conditions (such as high temperature heating for long period in inert atmosphere) and low surface area of electrides, limit their catalytic applications.[53,96] Production of electrides with high surface active sites at industrial level needs much attention with new synthetic methods. The bulk intermetallic electride retains most of active Ru species not accessible for reactants and underrates activity with respect to active metal. Laser ablation, chemical

vapor deposition techniques are possible approaches that improve the active sites of bulk IM.[104] Recently, different CVD routes developed for synthesis of binary silicides, amongst Rochow process has industrially realized for decades and synthesis effort on LaCoSi or LaRuSi electrides through these techniques would put a step forward towards the industrial production with better catalytic active sites.[168] Ball milling adopted to convert bulk IMCs to nanomaterials with improved surface area is another option possible at industrial scale, but still suffers with non-uniform particle size.[96] Ru supported electrides are extremely studied at low pressure (0.1–1 MPa). For Ru/Ca12A7:e^-, TOF increases with pressure till 1 MPa, beyond this, TOF curve becomes independent of pressure, limiting their application only to very low pressure.[19] Catalytic activity, stability, and hydride storage capacity of electrides at high pressure (above 1 MPa) is mysterious for their commercial application at moderate reactor (2–5 MPa) and needs dedicated investigation.

The time frame for the acquirement of knowledge is truly remarkable, it took decades for Fe catalysts, but only 8–10 years for electrides, and takes few years for new oxy-nitride-hydride catalysts.[22] Unfortunately, ternary nitrides discovered 20 years back, considered as one of family of promising catalysts in NH_3 synthesis are still under establishment phase.[21] Until recently, several mechanistic aspects such as involvement of lattice N through Mars van Krevelen mechanism enlightened, much more persuasiveness of pioneering experiments should continue. Several newly developed quaternary and ternary nitrides of Ni and Fe, could not beat Co_3Mo_3N in a catalytic race. The new synthesis methodologies of ternary nitrides with nano size embedded on support should enhance surface active sites with new quantum confinement effect in catalysis compared to bulk nitride.[86] Synthetic approaches that combined binary nitrides with hydrides, eventually overcome deactivation of metal nitrides by N_2 and appear as alternative way for exploring ternary nitrides in this direction.[56]

The oxides are still promising support at industrial level due to their stable, easy synthesis and possible handling at large scale compared to electrides and hydride. The SMSI and morphology dependent studies on Lanthanum oxides support led to new ideas for of exploring novel oxygen deficient metal oxides with different compositions and morphologies in NH_3 synthesis.[169] Early investigation, on perovskites (with ABO_3 structure) as oxide supports for Ru catalysts, sounded of less interest with limited activity.[125] Until recently, formation of oxy-hydrides and oxy-nitride-hydrides in perovskite ($ABO_{3-x}H_yN_z$) structure created enormous curiosity compared to their oxide form with amazing NH_3 synthesize rate. $ABO_{3-x}H_yN_z$ follow completely different mechanistic pathway involving lattice hydride (H^-) and nitride (N^{3-}) through Mars van Krevelen mechanism demanding further exploration.[22] The wide possible variety A and B cations embedded in perovskite structure, allowing design of diverse engineered materials will assist in building a new platform of oxy-nitride-hydride catalysts for NH_3 synthesis.[170]

The structure sensitivity of ruthenium catalyst in NH_3 synthesis was attributed to the presence of B_5 sites, which are extremely active and dominate the reaction rate. The fraction of B_5 sites majorly depends on the crystal size of Ru and morphology of support, but nothing known about the effect of Ru crystal structure. Ru in all the supported catalysts crystallizes in hcp structure rather than metastable fcc crystal structure. Recently, with suitable supports fcc crystal structure with more efficient active B_5 sites improved the NH_3 synthesis rate.[133] Ru with fcc phase over supported catalysts is another fascinating research topic for itself, with different solutions exciting as synthesis methods.[171,172] High surface area (83 m^2/g), Ru nano-sponges with fcc crystal structure developed using a special reducing agent were superior in hydrogenation reactions.[172] Until recently, only B_5 sites in Ru were considered as active for N_2 activation. But several Ru based catalysts with special electronic and geometrical structures such as Ru_2Y, LaRuSi, single atom Ru in zeolite framework and Ru substituted ABO_3 perovskite, all without B_5 sites, still exhibited a significant activity in NH_3 synthesis with different pathways concluding presence of B_5 site is not always essential for development of Ru catalyst in NH_3 synthesis.[131,134]

Alternative to Ru, Co appears be the second metal that is active for N_2 activation provided an excellent support and promoter (electronic and structurally) and switch to new Co based catalysts could occur in near future.[34,40,149][131,173] Apart this there are several non-noble metal based catalysts such as TiH_2, Co–LiH/BaH_2, LaCoSi and $LaCoO_3$ that appears to be promising with their extensive hydride storage and superior N_2 activation in NH_3 synthesis. The discovery of new transition metal based catalyst with hydride as co-catalyst, on the other hand, opens many possibilities, especially when considering that NH_3 catalysis has been extensively explored for a century, but neither Ti, V, Cr, Mn nor Ni were identified as effective catalysts. Early transition metal elements, which are inactive for ammonia synthesis shows good activity, breaking the well-known scaling rules. Hydrides change the situation and appears to be promising with new innovative research direction in the future. Very recent studies also suggest LaN with transition metal like Ni can catalyzed NH_3 synthesis similar to Ru based catalyst generated more curiosity on these materials.

Most of the new catalysts studied recently were better in performance-compared to classical benchmark Cs–Ru/MgO and Ru/AC catalysts in NH_3 synthesis. Different synthesis and reaction conditions such as pressure, temperature, Ru loading and presence/absence of active Ru in catalyst creates difficulty to compare the proficiency of each catalysts. But after careful analysis, at low temperature (300–350 °C) and 0.1 MPa pressure, calcium based supported Ru catalysts such as CaH_2, Ca_2N:e^-,$Ca(NH_2)_2$, Ba/Ru/$LaCeO_3$ are promising. In case of non-Ru based catalysts, conventional mass-based aspect, the 3d metals-hydride (Co–BaH_2) catalysts are much more active than Co_3Mo_3N, and LaCoSi. Supported Fe–LiH and Co–BaH_2 are even superior to most of the Ru-based catalysts. After discovery of highly efficient electrides, hydrides, nitrides, perovskites, oxides based Ru catalysts; certainly, Cs–Ru/MgO is no more the benchmark catalyst. However, each of these catalysts have their own Pro and Cons in terms of commercialization related to bulk synthesis, cost of catalyst, stability, operating conditions and

finally potential profit. However, insights on the new materials and their mechanisms will dig towards finding a realistic catalyst for NH_3 synthesis. Therefore, process of finding new NH_3 synthesis catalyst will never end, and a new story with new catalytic mechanism will continue to grow in the future.

Acknowledgement

Vijaykumar S.M and E.M Gaigneaux are thankful to Marie Skłodowska Curie – Individual Fellowship (MSCA-IF-EF-ST), Horizon 2020 – Research and Innovation Framework Programmed, (Project number: 841964) for funding.

Conflict of Interest

The authors declare no conflict of interest.

Keywords: Ammonia · Electride · Nitride · Hydride · Oxide · Mechanism · Ruthenium

[1] S. L. Foster, S. I. P. Bakovic, R. D. Duda, S. Maheshwari, R. D. Milton, S. D. Minteer, M. J. Janik, J. N. Renner, L. F. Greenlee, *Nat. Can.* **2018**, *1*, 490–500.
[2] H. Liu, *Ammonia Synthesis Catalysts: Innovation and Practice*, World Scientific Publishing Company Pte Limited, **2013**, pp. 1–65.
[3] Q. Wang, J. Guo, P. Chen, *J. Energy Chem.* **2019**, *36*, 25–36.
[4] H. Liu, Chin . *J. Catal.* **2014**, *35*, 1619–1640.
[5] G. Ertl, *Catal. Rev.* **1980**, *21*, 201–223.
[6] T. H. Rod, A. Logadottir, J. K. Nørskov, *J. Chem. Phys.* **2000**, *112*, 5343–5347.
[7] R. Schlögl, *Angew. Chem. Int. Ed.* **2003**, *42*, 2004–2008; *Angew. Chem.* **2003**, *115*, 2050–2055.
[8] W. Raróg-Pilecka, E. Miśkiewicz, S. Jodzis, J. Petryk, D. Łomot, Z. Kaszkur, Z. Karpiński, Z. Kowalczyk, *J. Catal.* **2006**, *239*, 313–325.
[9] C. Leterme, C. Fernández, P. Eloy, E. M. Gaigneaux, P. Ruiz, *Catal. Today.* **2017**, *286*, 85–100.
[10] C. Fernández, N. Bion, E. M. Gaigneaux, D. Duprez, P. Ruiz, *J. Catal.* **2016**, *344*, 16–28.
[11] S. Dahl, A. Logadottir, R. C. Egeberg, J. H. Larsen, I. Chorkendorff, E. Törnqvist, J. K. Nørskov, *Phys. Rev. Lett.* **1999**, *83*, 1814–1817.
[12] K. Honkala, A. Hellman, I. N. Remediakis, A. Logadottir, A. Carlsson, S. Dahl, C. H. Christensen, J. K. Nørskov, *Science.* **2005**, *307*, 555–558.
[13] C. J. H. Jacobsen, S. Dahl, P. L. Hansen, E. Törnqvist, L. Jensen, H. Topsøe, D. V. Prip, P. B. Møenshaug, I. Chorkendorff, *J. Mol. Catal. A* **2000**, *163*, 19–26.
[14] K. Aika, A. Ohya, A. Ozaki, Y. Inoue, I. Yasumori, *J. Catal.* **1985**, *92*, 305–311.
[15] K.i. Aika, *Angew. Chem. Int. Ed. Engl.* **1986**, *25*, 558–559.
[16] N. Saadatjou, A. Jafari, S. Sahebdelfar, *Chem. Eng. Commun.* **2015**, *202*, 420–448.
[17] D. Szmigiel, H. Bielawa, M. Kurtz, O. Hinrichsen, M. Muhler, W. Raróg, S. Jodzis, Z. Kowalczyk, L. Znak, J. Zieliński, *J. Catal.* **2002**, *205*, 205–212.
[18] Y. V. Larichev, B. L. Moroz, V. I. Zaikovskii, S. M. Yunusov, E. S. Kalyuzhnaya, V. B. Shur, V. I. Bukhtiyarov, *J. Phys. Chem. C.* **2007**, *111*, 9427–9436.
[19] M. Kitano, Y. Inoue, Y. Yamazaki, F. Hayashi, S. Kanbara, S. Matsuishi, T. Yokoyama, S. W. Kim, M. Hara, H. Hosono, *Nat. Chem.* **2012**, *4*, 934–940.
[20] C. Liu, S. A. Nikolaev, W. Ren, L. A. Burton, *J. Mater. Chem. C.* **2020**, *8*, 10551-10567 .
[21] J. S. J. Hargreaves, *Appl. Petrochem. Res.* 2014, 4, 3–10.
[22] M. Kitano, J. Kujirai, K. Ogasawara, S. Matsuishi, T. Tada, H. Abe, Y. Niwa, H. Hosono, *J. Am. Chem. Soc.* **2019**, *141*, 20344–20353.
[23] A. Nielsen, *Catal. Rev.*, **1971**, *4*, 1–26.
[24] M. Hara, M. Kitano, H. Hosono, *ACS Catal.* **2017**, *7*, 2313–2324.
[25] J. S. J. Hargreaves, *Hydrogenation, 7. Heterogeneously catalyzed ammonia synthesis*, De Gruyter, **2018**, pp. 173–192..
[26] W. Gao, J. Guo, P. Chen, *Chin. J. Chem.* **2019**, *37*, 442–451.
[27] J. L. Dye, *Acc. Chem. Res.* **2009**, *42*, 1564–1572.
[28] S. Matsuishi, Y. Toda, M. Miyakawa, K. Hayashi, T. Kamiya, M. Hirano, I. Tanaka, H. Hosono, *Science.* **2003**, *301*, 626–629.
[29] Y. Toda, Y. Kubota, M. Hirano, H. Hirayama, H. Hosono, *ACS Nano.* **2011**, *5*, 1907–1914.
[30] P. V. Sushko, A. L. Shluger, K. Hayashi, M. Hirano, H. Hosono, *Phys. Rev. Lett.* **2003**, *91*, 126401.
[31] S. Kanbara, M. Kitano, Y. Inoue, T. Yokoyama, M. Hara, H. Hosono, *J. Am. Chem. Soc.* **2015**, *137*, 14517–14524.
[32] M. Kitano, S. Kanbara, Y. Inoue, N. Kuganathan, P. V. Sushko, T. Yokoyama, M. Hara, H. Hosono, *Nat. Commun.* **2015**, *6*, 6731–6739.
[33] Y. Inoue, M. Kitano, S. W. Kim, T. Yokoyama, M. Hara, H. Hosono, *ACS Catal.* **2014**, *4*, 674–680.
[34] Y. Inoue, M. Kitano, M. Tokunari, T. Taniguchi, K. Ooya, H. Abe, Y. Niwa, M. Sasase, M. Hara, H. Hosono, *ACS Catal.* **2019**, *9*, 1670–1679.
[35] J. Li, M. Kitano, T. N. Ye, M. Sasase, T. Yokoyama, H. Hosono, *ChemCatChem.* **2017**, *9*, 3078–3083.
[36] M. Kitano, Y. Inoue, H. Ishikawa, K. Yamagata, T. Nakao, T. Tada, S. Matsuishi, T. Yokoyama, M. Hara, H. Hosono, *Chem. Sci.* **2016**, *7*, 4036–4043.
[37] M. Hattori, T. Mori, T. Arai, Y. Inoue, M. Sasase, T. Tada, M. Kitano, T. Yokoyama, M. Hara, H. Hosono, *ACS Catal.* **2018**, *8*, 10977–10984.
[38] Y. Lu, J. Li, T. Tada, Y. Toda, S. Ueda, T. Yokoyama, M. Kitano, H. Hosono, *J. Am. Chem. Soc.* **2016**, *138*, 3970–3973.
[39] J. Wu, Y. Gong, T. Inoshita, D. C. Fredrickson, J. Wang, Y. Lu, M. Kitano, H. Hosono, *Adv. Mater.* **2017**, *29*, 1700924–1700931.
[40] Y. Gong, J. Wu, M. Kitano, J. Wang, T.-N. Ye, J. Li, Y. Kobayashi, K. Kishida, H. Abe, Y. Niwa, H. Yang, T. Tada, H. Hosono, *Nat. Can.* **2018**, *1*, 178–185.
[41] J. Wu, J. Li, Y. Gong, M. Kitano, T. Inoshita, H. Hosono, *Angew. Chem. Int. Ed.* **2019**, *58*, 825–829.
[42] J. Li, J. Wu, H. Wang, Y. Lu, T. Ye, M. Sasase, X. Wu, M. Kitano, T. Inoshita, H. Hosono, *Chem. Sci.* **2019**, *10*, 5712–5718.
[43] S. Murata, K. I. Aika, *Appl. Catal. A* **1992**, *82*, 1–12.
[44] S. Murata, K. I. Aika, *J. Catal.* **1992**, *136*, 110–117.
[45] Y. J. Kim, S. M. Kim, H. Hosono, J. W. Yang, S. W. Kim, *Chem. Commun.* **2014**, *50*, 4791–4794.
[46] K. Lee, S. W. Kim, Y. Toda, S. Matsuishi, H. Hosono, *Nature*, **2013**, *494*, 336–340.
[47] Y. J. Kim, S. M. Kim, E. J. Cho, H. Hosono, J. W. Yang, S. W. Kim, *Chem. Sci.* **2015**, *6*, 3577–3581.
[48] H. Abe, Y. Niwa, M. Kitano, Y. Inoue, M. Sasase, T. Nakao, T. Tada, T. Yokoyama, M. Hara, H. Hosono, *J. Phys. Chem. C.* **2017**, *121*, 20900–20904.
[49] T. Nakao, T. Tada, H. Hosono, *J. Phys. Chem. C.* **2020**, *124*, 2070–2078.
[50] P. V. Ong, L. E. Johnson, H. Hosono, P. V. Sushko, *J. Mater. Chem. A.* **2017**, *5*, 5550–5558.
[51] W. Gao, P. Wang, J. Guo, F. Chang, T. He, Q. Wang, G. Wu, P. Chen, *ACS Catal.* **2017**, *7*, 3654–3661.
[52] T. Nakao, T. Tada, H. Hosono, *J. Phys. Chem. C.* **2020**, *124*, 1529–1534.
[53] T. Takeshita, W. E. Wallace, R. S. Craig, *J. Catal.* **1976**, *44*, 236–243.
[54] J. R. Norton, J. Sowa, *Chem. Rev.* **2016**, *116*, 8315–8317.
[55] S. F. Matar, *Prog. Solid State Chem.* **2010**, *38*, 1–37.
[56] P. Wang, F. Chang, W. Gao, J. Guo, G. Wu, T. He, P. Chen, *Nat. Chem.* **2017**, *9*, 64–70.
[57] F. Chang, Y. Guan, X. Chang, J. Guo, P. Wang, W. Gao, G. Wu, J. Zheng, X. Li, P. Chen, *J. Am. Chem. Soc.* **2018**, *140*, 14799–14806.
[58] P. Wang, H. Xie, J. Guo, Z. Zhao, X. Kong, W. Gao, F. Chang, T. He, G. Wu, M. Chen, L. Jiang, P. Chen, *Angew. Chem. Int. Ed.* **2017**, *56*, 8716–8720; *Angew. Chem.* **2017**, *129*, 8842–8846.
[59] Y. Kobayashi, Y. Tang, T. Kageyama, H. Yamashita, N. Masuda, S. Hosokawa, H. Kageyama, *J. Am. Chem. Soc.* **2017**, *139*, 18240–18246.
[60] Y. Tang, Y. Kobayashi, N. Masuda, Y. Uchida, H. Okamoto, T. Kageyama, S. Hosokawa, F. Loyer, K. Mitsuhara, K. Yamanaka, Y. Tamenori, C. Tassel, T. Yamamoto, T. Tanaka, H. Kageyama, *Met. Adv. Energy Mater.* **2018**, *8*, 1801772.
[61] H. Yamashita, T. Broux, Y. Kobayashi, F. Takeiri, H. Ubukata, T. Zhu, M. A. Hayward, K. Fujii, M. Yashima, K. Shitara, A. Kuwabara, T. Murakami, H. Kageyama, *J. Am. Chem. Soc.* **2018**, *140*, 11170–11173.
[62] M. Hattori, S. Iijima, T. Nakao, H. Hosono, M. Hara, *Nat. Commun.* **2020**, *11*, 2001.

[63] N. Segal, F. Sebba, *J. Catal.* **1967**, *8*, 105–112.
[64] N. Segal, F. Sebba, *J. Catal.* **1967**, *8*, 113–119.
[65] D. A. King, F. Sebba, *J. Catal.* **1965**, *4*, 253–259.
[66] G. I. Panov, A. S. Kharitonov, *React. Kinet. Catal. Lett.* **1985**, *29*, 267–274.
[67] R. Kojima, K.i. Aika, *Appl. Catal. A* **2001**, *209*, 317–325.
[68] J. S. J. Hargreaves, *Coord. Chem. Rev.* **2013**, *257*, 2015–2031.
[69] R. Kojima, K.i. Aika, *Appl. Catal. A* **2001**, *215*, 149–160.
[70] R. Kojima, K.i. Aika, *Appl. Catal. A* **2001**, *218*, 121–128.
[71] C. J. H. Jacobsen, *Chem. Commun.* **2000**, 1057–1058.
[72] R. Kojima, K.i. Aika, *Appl. Catal. A* **2001**, *219*, 157–170.
[73] A. Boisen, S. Dahl, C. J. H. Jacobsen, *J. Catal.* **2002**, *208*, 180–186.
[74] C. J. H. Jacobsen, S. Dahl, B. S. Clausen, S. Bahn, A. Logadottir, J. K. Nørskov, *J. Am. Chem. Soc.* **2001**, *123*, 8404–8405.
[75] S. Dahl, A. Logadottir, C. J. H. Jacobsen, J. K. Nørskov, *Appl. Catal. A* **2001**, *222*, 19–29.
[76] D. McKay, D. H. Gregory, J. S. J. Hargreaves, S. M. Hunter, X. Sun, *Chem. Commun.* **2007**, 3051–3053.
[77] J. S. J. Hargreaves, D. McKay, *J. Mol. Catal. A* **2009**, *305*, 125–129.
[78] D. H. Gregory, J. S. J. Hargreaves, S. M. Hunter, *Catal. Lett.* **2011**, *141*, 22–26.
[79] S. M. Hunter, D. McKay, R. I. Smith, J. S. J. Hargreaves, D. H. Gregory, *Chem. Mater.* **2010**, *22*, 2898–2907.
[80] S. M. Hunter, D. H. Gregory, J. S. J. Hargreaves, M. Richard, D. Duprez, N. Bion, *ACS Catal.* **2013**, *3*, 1719–1725.
[81] C. D. Zeinalipour-Yazdi, J. S. J. Hargreaves, C. R. A. Catlow, *J. Phys. Chem. C.* **2015**, *119*, 28368–28376.
[82] J. Moellmann, S. Grimme, *J. Phys. Chem. C.* **2014**, *118*, 7615–7621.
[83] C. D. Zeinalipour-Yazdi, J. S. J. Hargreaves, C. R. A. Catlow, *J. Phys. Chem. C.* **2018**, *122*, 6078–6082.
[84] N. Bion, F. Can, J. Cook, J. S. J. Hargreaves, A. L. Hector, W. Levason, A. R. McFarlane, M. Richard, K. Sardar, *Appl. Catal. A* **2015**, *504*, 44–50.
[85] M. Y. Aslan, J. Hargreaves, D. Uner , *Faraday Discuss.* **2020**.
[86] Y. Tsuji, M. Kitano, K. Kishida, M. Sasase, T. Yokoyama, M. Hara, H. Hosono, *Chem. Commun.* **2016**, *52*, 14369–14372.
[87] I. AlShibane, A. Daisley, J. S. J. Hargreaves, A. L. Hector, S. Laassiri, J. L. Rico, R. I. Smith, *ACS Sustainable Chem. Eng.* **2017**, *5*, 9214–9222.
[88] A. Daisley, J. S. J. Hargreaves, *J. Energy Chem.* **2019**, *39*, 170–175.
[89] M. AlShalwi, J. S. J. Hargreaves, J. J. Liggat, *D. Mater. Res. Bull.* **2012**, *47*, 1251–1256.
[90] S. Alconchel, F. Sapiña, D. Beltrán, A. Beltrán, *J. Mater. Chem.* **1998**, *8* 1901–1909.
[91] S. Al Sobhi, J. S. J. Hargreaves, A. L. Hector, S. Laassiri, *Dalton Trans.* **2019**, *48*, 16786–16792.
[92] A. M. Alexander, J. S. J. Hargreaves, C. Mitchell, *Top. Catal.* **2012**, *55*, 1046–1053.
[93] K. McAulay, J. S. J. Hargreaves, A. R. McFarlane, D. J. Price, N. A. Spencer, N. Bion, F. Can, M. Richard, H. F. Greer, W. Z. Zhou, *Catal. Commun.* **2015**, *68*, 53–57.
[94] T. N. Ye, S. W. Park, Y. Lu, J. Li, M. Sasase, M. Kitano, T. Tada, H. Hosono, *Nature*, **2020**, *583*, 391–395.
[95] L. Li, T. Zhang, J. Cai, H. Cai, J. Ni, B. Lin, J. Lin, X. Wang, L. Zheng, C.-T. Au, L. Jiang, *J. Catal.* **2020**, *389*, 218–228.
[96] V. S. Marakatti, S. C. Peter, *Prog. Solid State Chem.* **2018**, *52*, 1–30.
[97] V. S. Marakatti, S. C. Sarma, S. Sarkar, M. Krajčí, E. M. Gaigneaux, S. C. Peter, *ACS Appl. Mater. Interfaces.* **2019**, *11*, 37602–37616.
[98] V. S. Marakatti, N. Arora, S. Rai, S. C. Sarma, S. C. Peter, *ACS Sustainable Chem. Eng.* **2018**, *6*, 7325–7338.
[99] V. S. Marakatti, S. C. Sarma, B. Joseph, D. Banerjee, S. C. Peter, *ACS Appl. Mater. Interfaces.* **2017**, *9*, 3602–3615.
[100] V. S. Marakatti, S. C. Peter, *New J. Chem.* **2016**, *40*, 5448–5457.
[101] K. Urabe, T. Yoshioka, A. Ozaki, *J. Catal.* **1978**, *54*, 52–56.
[102] B. Rudolf, O. Yoshio, *Bull. Chem. Soc. Jpn.* **1966**, *39*, 1678–1681.
[103] T. Hikita, K.i. Aika, T. Onishi, *Catal. Lett.* **1990**, *4*, 157–161.
[104] T. Ogawa, Y. Kobayashi, H. Mizoguchi, M. Kitano, H. Abe, T. Tada, Y. Toda, Y. Niwa, H. Hosono, *J. Phys. Chem. C.* **2018**, *122*, 10468–10475.
[105] X. L. Ma, J. C. Liu, H. Xiao, J. Li, *J. Am. Chem. Soc.* **2018**, *140*, 46–49.
[106] K. K. Ghuman, K. Tozaki, M. Sadakiyo, S. Kitano, T. Oyabe, M. Yamauchi, *Phys. Chem. Chem. Phys.* **2019**, *21*, 5117–5122.
[107] A. R. Cholach, *Appl. Catal. A* **2018**, *562*, 223–233.
[108] Q. An, Y. Shen, A. Fortunelli, W. A. Goddard, *J. Am. Chem. Soc.* **2018**, *140*, 17702–17710.
[109] Y. Niwa, K.i. Aika, *J. Catal.* **1996**, *162*, 138–142.
[110] Z. Ma, S. Zhao, X. Pei, X. Xiong, B. Hu, *Catal. Sci. Technol.* **2017**, *7*, 191–199.
[111] B. Lin, Y. Liu, L. Heng, X. Wang, J. Ni, J. Lin, L. Jiang, *Ind. Eng. Chem. Res.* **2018**, *57*, 9127–9135.
[112] W. Li, P. Liu, R. Niu, J. Li, S. Wang, *Solid State Sci.* **2020**, *99*, 105983.
[113] Z. Ma, X. Xiong, C. Song, B. Hu, W. Zhang, *RSC Adv.* **2016**, *6*, 51106–51110.
[114] Y. Wu, C. Li, B. Fang, X. Wang, J. Ni, B. Lin, J. Lin, L. Jiang, *Chem. Commun.* **2020**, *56*, 1141–1144.
[115] W. Han, Z. Li, H. Liu, *J. Rare Earths.* **2019**, *37*, 492–499.
[116] M. Malmali, Y. Wei, A. McCormick, E. L. Cussler, *Ind. Eng. Chem. Res.* **2016**, *55*, 8922–8932.
[117] Y. Ogura, K. Sato, S.i. Miyahara, Y. Kawano, T. Toriyama, T. Yamamoto, S. Matsumura, S. Hosokawa, K. Nagaoka, *Chem. Sci.* **2018**, *9*, 2230–2237.
[118] K. Sato, S.i. Miyahara, Y. Ogura, K. Tsujimaru, Y. Wada, T. Toriyama, T. Yamamoto, S. Matsumura, K. Nagaoka, *ACS Sustainable Chem. Eng.* **2020**, *8*, 2726–2734.
[119] K. Sato, K. Imamura, Y. Kawano, S.i. Miyahara, T. Yamamoto, S. Matsumura, K. Nagaoka, *Chem. Sci.* **2017**, *8*, 674–679.
[120] K. Imamura, S.i. Miyahara, Y. Kawano, K. Sato, Y. Nakasaka, K. Nagaoka, *J. Inst. Chem.* **2019**, *105*, 50–56.
[121] Y. Ogura, K. Tsujimaru, K. Sato, S.i. Miyahara, T. Toriyama, T. Yamamoto, S. Matsumura, K. Nagaoka, *ACS Sustainable Chem. Eng.* **2018**, *6*, 17258–17266.
[122] X. Wang, L. Li, T. Zhang, B. Lin, J. Ni, C. T. Au, L. Jiang , *Chem. Commun.* **2019**, *55*, 474–477.
[123] F. Kosaka, T. Nakamura, A. Oikawa, J. Otomo, *ACS Sustainable Chem. Eng.* **2017**, *5*, 10439–10446.
[124] Y. Horiuchi, G. Kamei, M. Saito, M. Matsuoka, *Chem. Lett.* **2013**, *42*, 1282–1284.
[125] X. L. Yang, W. Q. Zhang, C. G. Xia, X. M. Xiong, X. Y. Mu, B. Hu, *Catal. Commun.* **2010**, *11*, 867–870.
[126] Z. Wang, B. Liu, J. Lin, *Appl. Catal. A* **2013**, *458*, 130–136.
[127] N. Shimoda, Y. Kimura, Y. Kobayashi, J. Kubota, S. Satokawa, *Int. J. Hydrogen Energy.* **2017**, *42*, 29745–29755.
[128] W. Li, S. Wang, J. Li, *Chem. Asian J.* **2019**, *14*, 2815–2821.
[129] X. Yang, C. Xia, X. Xiong, X. Mu, B. Hu, *Chin. J. Catal.* **2010**, *31*, 377–379.
[130] L. Li, L. Yang, T. Zhang, X. Wang, X. Zhang, B. Lin, J. Ni, H. Dai, C. T. Au, L. Jiang, *Catal. Sci. Technol.* **2019**, *9*, 6217–6221.
[131] X. Wang, X. Peng, H. Ran, B. Lin, J. Ni, J. Lin, L. Jiang, *Ind. Eng. Chem. Res.* **2018**, *57*, 17375–17383.
[132] M. Chen, M. Yuan, J. Li, Z. You, *Appl. Catal. A* **2018**, *554*, 1–9.
[133] Y. Inoue, M. Kitano, K. Kishida, H. Abe, Y. Niwa, M. Sasase, Y. Fujita, H. Ishikawa, T. Yokoyama, M. Hara, H. Hosono, *ACS Catal.* **2016**, *6*, 7577–7584.
[134] J.-Z. Qiu, J. Hu, J. Lan, L. F. Wang, G. Fu, R. Xiao, B. Ge, J. Jiang, *Chem. Mater.* **2019**, *31*, 9413–9421.
[135] K. Kishida, M. Kitano, M. Sasase, P. V. Sushko, H. Abe, Y. Niwa, K. Ogasawara, T. Yokoyama, H. Hosono, *ACS Appl. Energy Mater.* **2020**, *3*, 6573–6582 .
[136] D. E. Brown, T. Edmonds, R. W. Joyner, J. J. McCarroll, S. R. Tennison, *Catal. Lett.* **2014**, *144*, 545–552.
[137] H. B. Chen, J. D. Lin, Y. Cai, X. Y. Wang, J. Yi, J. Wang, G. Wei, Y. Z. Lin, D. W. Liao, *Appl. Surf. Sci.* **2001**, *180*, 328–335.
[138] B. Lin, K. Wei, *Catal. Commun.* **2013**, *41*, 110–114.
[139] C. Liang, Z. Wei, Q. Xin, C. Li, *React. Kinet. Catal. Lett.* **2004**, *83*, 39–45.
[140] C. Liang, Z. Wei, M. Luo, P. Ying, Q. Xin, C. Li, *Stud. Surf. Sci. Catal.* (Eds. A. Guerrero-Ruiz, I. Rodríguez-Ramos) Elsevier, **2001**, pp. 283–290.
[141] H. Liang, G. Chen, S. Desinan, R. Rosei, F. Rosei, D. Ma, *Int. J. Hydrogen Energy.* **2012**, *37*, 17921–17927.
[142] M. Nishi, S. Y. Chen, H. Takagi, *Sustainable Energy Fuels.* **2020**, *4*, 832–842.
[143] C. Liang, Z. Li, J. Qiu, C. Li, *J. Catal.* **2002**, *211*, 278–282.
[144] Z. Ma, S. Zhao, X. Xiong, B. Hu, C. Song, *Catal. Lett.* **2016**, *146*, 2324–2329.
[145] W. Han, H. Liu, H. Zhu, *Catal. Commun.* **2007**, *8*, 351–354.
[146] Y. Li, C. Pan, W. Han, H. Chai, H. Liu, *Catal. Today.* **2011**, *174*, 97–105.
[147] J. Ni, R. Wang, J. Lin, K. Wei, *Catal. Lett.* **2008**, *126*, 134–141.
[148] C. Zhou, Y. Zhu, H. Liu, *J. Rare Earths.* **2010**, *28*, 552–555.
[149] A. Tarka, M. Zybert, E. Truszkiewicz, B. Mierzwa, L. Kępiński, D. Moszyński, W. Raróg-Pilecka, *ChemCatChem.* **2015**, *7*, 2836–2839.
[150] B. Lin, Y. Guo, C. Cao, J. Ni, J. Lin, L. Jiang, *Catal. Today.* **2018**, *316*, 230–236.
[151] B. Lin, Y. Qi, Y. Guo, J. Lin, J. Ni, *Catal. Sci. Technol.* **2015**, *5*, 2829–2838.
[152] J. Ni, J. Lin, X. Wang, B. Lin, J. Lin, L. Jiang, *ChemistrySelect.* **2017**, *2*, 6040–6046.

[153] M. Nishi, S. Y. Chen, H. Takagi, *ChemCatChem.* **2018**, *10*, 3411–3414.
[154] M. Nishi, S. Y. Chen, H. Takagi, *Catalysts.* **2019**, *9*, 406–427.
[155] Y. Zhou, Y. Ma, G. Lan, H. Tang, W. Han, H. Liu, Y. Li, *A Chin. J. Catal.* **2019**, *40*, 114–123.
[156] Y. Ma, G. Lan, X. Wang, G. Zhang, W. Han, H. Tang, H. Liu, Y. Li, *RSC Adv.* **2019**, *9*, 22045–22052.
[157] I. Luz, S. Parvathikar, M. Carpenter, T. Bellamy, K. Amato, J. Carpenter, M. Lail, *Catal. Sci. Technol.* **2020**, *10*, 105–112.
[158] N. S. Smirnova, K. N. Iost, V. L. Temerev, T. I. Gulyaeva, M. V. Trenikhin, I. V. Muromtsev, E. V. Khramov, Y. V. Zubavichus, D. A. Shlyapin, P. G. Tsyrul'nikov, *Mol. Catal.* **2017**, *433*, 235–241.
[159] B. Lin, L. Heng, H. Yin, B. Fang, J. Ni, X. Wang, J. Lin, L. Jiang, *Ind. Eng. Chem. Res.* **2019**, *58*, 10285–10295.
[160] M. Kitano, Y. Inoue, M. Sasase, K. Kishida, Y. Kobayashi, K. Nishiyama, T. Tada, S. Kawamura, T. Yokoyama, M. Hara, H. Hosono, *Angew. Chem. Int. Ed.* **2018**, *57*, 2648–2652; *Angew. Chem.* **2018**, *130*, 2678–2682.
[161] V. S. Marakatti, P. V. C. Rao, N. V. Choudary, G. S. Ganesh, G. Shah, S. P. Maradur, A. B. Halgeri, G. V. Shanbhag, R. Ravishankar, Influence of Alkaline Earth Cation Exchanged X-Zeolites Towards Ortho-Selectivity in Alkylation of Aromatics: Hard-Soft-Acid-Base Concept, *Adv. Porous Mater.* **2014**, *2* 221–229.
[162] C. T. Fishel, R. J. Davis, J. M. Garces, *J. Catal.* **1996**, *163*, 148–157.
[163] B. C. McClaine, S. E. Siporin, R. J. Davis, *J. Phys. Chem. B.* **2001**,*105* 7525–7532.
[164] S. E. Siporin, B. C. McClaine, S. L. Anderson, R. J. Davis, *Catal. Lett.* **2002**, *81*, 265–269.
[165] I. Matito-Martos, J. García-Reyes, A. Martin-Calvo, D. Dubbeldam, S. Calero, *J. Phys. Chem. C.* **2019**, *123*, 18475–18481.
[166] F. Cuevas, J. M. Joubert, M. Latroche, A. Percheron-Guégan, *Appl. Phys. A.* **2001**, *72*, 225–238.
[167] S. Gupta, K. G. Suresh, *J. Alloys Compd.* **2015**, *618*, 562–606.
[168] X. Chen, C. Liang, *Catal. Sci. Technol.* **2019**, *9*, 4785–4820.
[169] L. Wang, X. Xie, K. N. Dinh, Q. Yan, J. Ma, *Coord. Chem. Rev.* **2019**, *397*, 138–167.
[170] S. Royer, D. Duprez, F. Can, X. Courtois, C. Batiot-Dupeyrat, S. Laassiri, H. Alamdari, *Chem. Rev.* **2014**, *114*, 10292–10368.
[171] K. Kusada, H. Kobayashi, T. Yamamoto, S. Matsumura, N. Sumi, K. Sato, K. Nagaoka, Y. Kubota, H. Kitagawa, *J. Am. Chem. Soc.* **2013**, *135*, 5493–5496.
[172] S. Ghosh, B. R. Jagirdar, *ChemCatChem.* **2018**, *10*, 3086–3095.
[173] H. Ronduda, M. Zybert, W. Patkowski, A. Tarka, P. Jodłowski, L. Kępiński, A. Sarnecki, D. Moszyński, W. Raróg-Pilecka, *Appl. Catal. A* **2020**, *598*, 117553–117568.

Manuscript received: July 13, 2020
Revised manuscript received: August 10, 2020
Accepted manuscript online: August 10, 2020
Version of record online: ■■, ■■■

REVIEWS

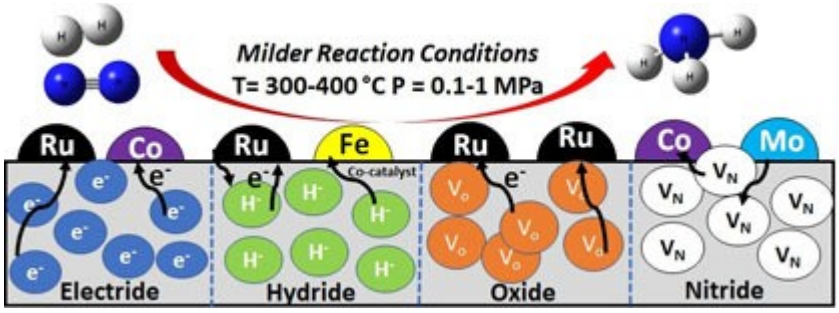

Dr. V. S. Marakatti, Prof. E. M. Gaigneaux*

TOC: This review will give insights on recent development in advanced materials such as electrides, hydrides, nitrides, oxides and oxy-hydrides-nitrides as support and active component of Ru based catalyst in NH_3 synthesis at milder reaction conditions. Electrides, hydrides, nitrides and oxides with their promising unique properties of reversible electron, hydride, nitride and oxide vacancies storage have tremendously improved Ru based catalysts efficiency. Perceptions on these materials and their mechanism digs towards finding a realistic catalyst for NH_3 synthesis.